(12) INTERNATIONAL APPLICATION PUBLISHED UNDER THE PATENT COOPERATION TREATY (PCT)

(19) World Intellectual Property Organization
International Bureau

(43) International Publication Date
25 May 2001 (25.05.2001)

PCT

(10) International Publication Number
WO 01/37309 A1

(51) International Patent Classification[7]: H01J 35/20, H01S 3/00, 3/22

(21) International Application Number: PCT/US00/29750

(22) International Filing Date: 26 October 2000 (26.10.2000)

(25) Filing Language: English

(26) Publication Language: English

(30) Priority Data:

09/442,582	18 November 1999 (18.11.1999)	US
09/590,962	9 June 2000 (09.06.2000)	US
09/690,084	16 October 2000 (16.10.2000)	US

(71) Applicants: CYMER, INC. [US/US]; 16750 Via Del Campo Court, San Diego, CA 92127-1712 (US). Birx, Deborah (executrix for the deceased inventor) [US/US]; 8505 White Post Court, Potomac, MD 20854, us (US).

(72) Inventors: PARTLO, William, N.; 12634 Pedriza Street, Poway, CA 92064 (US). FOMENKOV, Igor, V.; 14390 Janal Way, San Diego, CA 92129 (US). OLIVER, I., Roger; 3944 Carson Street, San Diego, CA 92117 (US). NESS, Richard, M.; 9248 Citrus View Court, San Diego, CA 92126 (US). BIRX, Daniel, L. (deceased).

(74) Agent: ROSS, John, R.; Cymer, Inc., Legal Department - MS/3-2A, 16750 Via Del Campo Court, San Diego, CA 92127-1712 (US).

(81) Designated States *(national)*: AE, AG, AL, AM, AT, AU, AZ, BA, BB, BG, BR, BY, BZ, CA, CH, CN, CR, CU, CZ, DE, DK, DM, DZ, EE, ES, FI, GB, GD, GE, GH, GM, HR, HU, ID, IL, IN, IS, JP, KE, KG, KP, KR, KZ, LC, LK, LR, LS, LT, LU, LV, MA, MD, MG, MK, MN, MW, MX, MZ, NO, NZ, PL, PT, RO, RU, SD, SE, SG, SI, SK, SL, TJ, TM, TR, TT, TZ, UA, UG, UZ, VN, YU, ZA, ZW.

(84) Designated States *(regional)*: ARIPO patent (GH, GM, KE, LS, MW, MZ, SD, SL, SZ, TZ, UG, ZW), Eurasian patent (AM, AZ, BY, KG, KZ, MD, RU, TJ, TM), European patent (AT, BE, CH, CY, DE, DK, ES, FI, FR, GB, GR, IE, IT, LU, MC, NL, PT, SE), OAPI patent (BF, BJ, CF, CG, CI, CM, GA, GN, GW, ML, MR, NE, SN, TD, TG).

Published:
— *With international search report.*

[Continued on next page]

(54) Title: PLASMA FOCUS LIGHT SOURCE WITH IMPROVED PULSE POWER SYSTEM

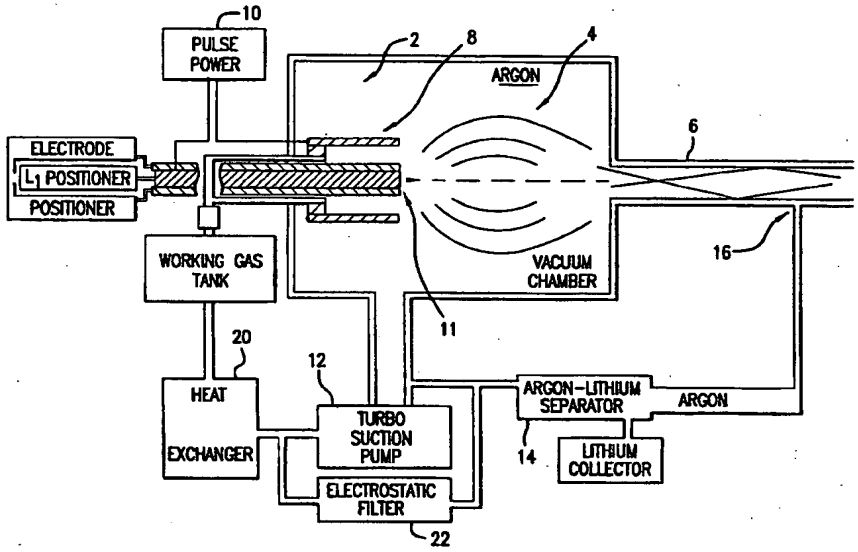

(57) Abstract: A high energy photon source. A pair of plasma pinch electrodes (8) are located in a vacuum chamber in a plasma pinch unit (2). The chamber contains a working gas which includes a noble buffer gas and an active gas chosen to produce a desired spectral line. A pulse power source (10) provides electrical pulses at high enough voltages to create electrical discharges between the electrodes. This produces high temperature, high density plasma pinches in the working gas providing radiation at the spectral line of the source. The electrodes are configured coaxially with the anode on the axis. Active gas is introduced through the hollow anode. This permits an optimization of the spectral line source and a separate optimization of the buffer gas.

WO 01/37309 A1

For two-letter codes and other abbreviations, refer to the "Guidance Notes on Codes and Abbreviations" appearing at the beginning of each regular issue of the PCT Gazette.

PLASMA FOCUS LIGHT SOURCE WITH IMPROVED PULSE POWER SYSTEM

This application is a continuation-in-part of U.S. Serial No. 09/590,962, filed June 9, 2000, U.S. Serial No. 09/442,582, filed November 18, 1999 and U.S. Serial No. 09/324,526, filed June 2, 1999 which was a continuation-in-part of U.S. Serial No. 09/268,243 filed March 15, 1999 now U.S. Patent No. 6,064,072 and U.S. Serial No. 09/093,416, filed June 8, 1998 now U.S. Patent No. 6,051,841 which was a CIP of Serial No. 08/854,507 which is now U.S. Patent No. 5,763,930. This invention relates to high energy photon sources and in particular highly reliable x-ray and high energy ultraviolet sources.

BACKGROUND OF THE INVENTION

The semiconductor industry continues to develop lithographic technologies which can print ever smaller integrated circuit dimensions. These systems must have high reliability, cost effective throughput, and reasonable process latitude. The integrated circuit fabrication industry has recently changed over from mercury G-line (436 nm) and I-line (365 nm) exposure sources to 248 nm and 193nm excimer laser sources. This transition was precipitated by the need for higher lithographic resolution with minimum loss in depth-of-focus.

The demands of the integrated circuit industry will soon exceed the resolution capabilities of 193nm exposure sources, thus creating a need for a reliable exposure source at a wavelength significantly shorter than 193nm. An excimer line exists at 157nm, but optical materials with sufficient transmission at this wavelength and sufficiently high optical quality are difficult to obtain. Therefore, all-reflective imaging systems may be required. An all reflective optical system requires a smaller numerical aperture than the transmissive systems. The loss in resolution caused by the smaller NA can only be made up by reducing the wavelength by a large factor. Thus, a light source in the range of 10nm is required if the resolution of optical lithography is to be improved beyond that achieved with 193 nm or 157 nm.

The present state of the art in high energy ultraviolet and x-ray sources utilizes plasmas produced by bombarding various target materials with laser beams, electrons or other particles. Solid targets have been used, but the debris created by ablation of the solid target has detrimental effects on various components of a system intended for production line operation. A proposed solution to the debris problem is to use a frozen liquid or frozen gas target so that the debris will not plate out onto the optical equipment. However, none of these systems have proven to be practical for production line operation.

It has been well known for many years that x-rays and high energy ultraviolet radiation could be produced in a plasma pinch operation. In a plasma pinch an electric current is passed through a plasma in one of several possible configuration such that the magnetic field created by the flowing electric current accelerates the electrons and ions in the plasma into a tiny volume with sufficient energy to cause substantial stripping of outer electrons from the ions and a consequent production of x-rays and high energy ultraviolet radiation. Various prior art techniques for generation of high energy radiation from focusing or pinching plasmas are described in the following patents:

·J.M. Dawson, "X-Ray Generator," *U.S. Patent #3,961,197*, June 1, 1976.

·T.G. Roberts, et. al., "Intense, Energetic Electron Beam Assisted X-Ray Generator," *U.S. Patent #3,969,628*, July 13, 1976.

·J.H. Lee, "Hypocycloidal Pinch Device,"*U.S. Patent #4,042,848*, Aug. 16, 1977.

·L. Cartz, et. al., "Laser Beam Plasma Pinch X-Ray System," *U.S. Patent #4,504,964*, Mar. 12, 1985.

·A. Weiss, et. al., "Plasma Pinch X-Ray Apparatus," *U.S. Patent #4,536,884*, Aug. 20, 1985.

·S. Iwamatsu, "X-Ray Source," *U.S. Patent #4,538,291*, Aug. 27, 1985.

·G. Herziger and W. Neff, "Apparatus for Generating a Source of Plasma with High Radiation Intensity in the X-ray Region, *"U.S. Patent No. 4,596,030*, June 17, 1986.

·A. Weiss, et. al, "X-Ray Lithography System," *U.S. Patent #4,618,971*, Oct. 21, 1986.

·A. Weiss, et. al., "Plasma Pinch X-ray Method," *U.S. Patent #4,633,492*, Dec. 30, 1986.

·I. Okada, Y. Saitoh, "X-Ray Source and X-Ray Lithography Method," *U.S. Patent #4,635,282*, Jan. 6, 1987.

·R.P. Gupta, et. al., "Multiple Vacuum Arc Derived Plasma Pinch X-Ray Source," *U.S. Patent #4,751,723,* June 14, 1988.

·R.P. Gupta, et. al., "Gas Discharge Derived Annular Plasma Pinch X-Ray Source," *U.S. Patent #4,752,946,* June 21, 1988.

·J.C. Riordan, J.S. Peariman, "Filter Apparatus for use with an X-Ray Source," *U.S. Patent #4,837,794,* June 6, 1989.

·W. Neff, et al., "Device for Generating X-radiation with a Plasma Source", *U.S. Patent #5,023,897*, June 11, 1991.

·D.A. Hammer, D.H. Kalantar, "Method and Apparatus for Microlithography Using X-Pinch X-Ray Source," *U.S. Patent #5,102,776*, April 7, 1992.

·M.W. McGeoch, "Plasma X-Ray Source," *U.S. Patent #5,504,795*, April 2, 1996.

·G. Schriever, et al., "Laser-produced Lithium Plasma as a Narrow-band Extended Ultraviolet Radiation Source for Photoelectron Spectroscopy", *Applied Optics*, Vol. 37, No. 7, pp. 1243-1248, March 1998.

·R. Lebert, et al., "A Gas Discharged Based Radiation Source for EUV Lithography", *Int. Conf. On Micro and Nano Engineering*, September, 1998.

·W. T. Silfast, et al., "High-power Plasma Discharge Source at 13.5nm and 11.4nm for EUV Lithography", *SPIE Proc. On Emerging Lithographic Technologies III*, Vol. 3676, pp. 272-275, March 1999.

·F. Wu, et al., "The Vacuum Spark and Spherical Pinch X-ray/EUV Point Sources", *SPIE Proc. On Emerging Lithographic Technologies III*, Vol. 3676, pp. 410-420, March 1999.

·I. Fomenkov, W. Partlo, D. Birx, "Characterization of a 13.5nm for EUV Lithography based on a Dense Plasma Focus and Lithium Emission", *Sematech International Workshop on EUV Lithography*, October, 1999.

Typical prior art plasma focus devices can generate large amounts of radiation suitable for proximity x-ray lithography, but are limited in repetition rate due to large per pulse

electrical energy requirements, and short lived internal components. The stored electrical energy requirements for these systems range from 1kJ to 100kJ. The repetition rates typically did not exceed a few pulses per second.

What is needed is a production line reliable, simple system for producing high energy ultraviolet and x-radiation which operates at high repetition rates and avoids prior art problems associated with debris formation.

SUMMARY OF THE INVENTION

The present invention provides a high energy photon source. A pair of plasma pinch electrodes are located in a vacuum chamber. The chamber contains a working gas which includes a noble buffer gas and an active gas chosen to provide a desired spectral line. A pulse power source provides electrical pulses at voltages high enough to create electrical discharges between the electrodes to produce very high temperature, high density plasma pinches in the working gas providing radiation at the spectral line of the source or active gas. Preferably the electrodes are configured co-axially with the anode on the axis. The anode is preferably hollow and the active gas is introduced through the anode. This permits an optimization of the spectral line source and a separate optimization of the buffer gas. Preferred embodiments present optimization of capacitance values, anode length and shape and preferred active gas delivery systems are disclosed. Preferred embodiments also include a pulse power system comprising a charging capacitor and a magnetic compression circuit comprising a pulse transformer. A heat pipe cooling system is described for cooling the central anode.
In preferred embodiments an external reflection radiation collector-director collects radiation produced in the plasma pinch and directs the radiation in a desired direction. Embodiments are described for producing a focused beam and a parallel beam. Also in preferred embodiments the active gas is lithium vapor and the buffer gas is helium and the radiation-collector is made of or coated with a material possessing high grazing incidence reflectivity. Good choices for the reflector material are molybdenum, palladium, ruthenium, rhodium, gold or tungsten.

In other preferred embodiments the buffer gas is argon and lithium gas is produced by vaporization of solid or liquid lithium located in a hole along the axis of the central

electrode of a coaxial electrode configuration. In preferred embodiments, debris is collected on a conical nested debris collector having surfaces aligned with light rays extending out from the pinch site and directed toward the radiation collector-director. The conical nested debris collector and the radiation collector-director are maintained at a temperature in the range of about 400°C which is above the melting point of lithium and substantially below the melting point of tungsten. Both tungsten and lithium vapor will collect on the debris collector but the lithium will evaporate off the debris collector and the collector-director whereas the tungsten will remain permanently on the debris collector and therefore does not collect on and degrade the reflectivity of the radiation collector-director. The reflection radiation collector-director and the conical nested debris collector could be fabricated together as one part or they could be separate parts aligned with each other and the pinch site.

A unique chamber window may be provided, if needed, which is designed to transmit EUV light and reflect lower energy light including visible light. This window is preferably a small diameter window comprised of extremely thin material such as silicon, zirconium or beryllium.

Applicants describe herein a third generation Dense Plasma Focus (DPF) prototype device constructed by Applicants and their fellow workers as a source for extreme ultraviolet (EUV) lithography employing an all-solid-state pulse power drive. Using the results from a vacuum grating spectrometer combined with measurements with a silicon photo diode, Applicants have found that substantial amounts of radiation within the reflectance band of Mo/Si mirrors can be generated using the 13.5nm emission line of doubly ionized Lithium. This prototype DPF converts 25J of stored electrical energy per pulse into approximately 0.76J of in-band 13.5nm radiation emitted into 4π steradians. The pulse repetition rate performance of this device has been investigated up to its DC power supply limit of 200Hz. No significant reduction in EUV output per pulse was found up to this repetition rate. At 200Hz, the measured pulse-to-pulse energy stability was σ=6% and no drop out pulses were observed. The electrical circuit and operation of this prototype DPF device is presented along with a description of several preferred modifications intended to improve stability, efficiency and performance.

Also described is a fourth generation DPF device capable of operation at 2,000 Hz which is capable of producing about 20 mJ per pulse of useful EUV radiation into 2 π steradians.

The present invention provides a practical implementation of EUV lithography in a reliable, high brightness EUV light source with emission characteristics well matched to the reflection band of the Mo/Si or Mo/Be mirror systems.

BRIEF DESCRIPTION OF THE DRAWINGS

FIG. 1 and 1A are drawings of high energy photon sources representing preferred embodiments of the present invention.

FIG. 2 is a drawing of a three-dimensional plasma pinch device with disk shaped electrodes.

FIG. 3 is a drawing of a fourth preferred embodiment of the present invention.

FIG. 4 is a preferred circuit diagram for a preferred embodiment of the present invention.

FIG. 5A is a drawing of a prototype unit built by Applicants and their fellow workers.

FIG. 5B is a cross section view showing the electrodes of the prototype with spark plug pre-ionizers.

FIGS. 5B1-5B6 are drawings showing the buildup of the plasma pinch.

FIG. 5C shows a cross section of the electrode region with the addition of a blast shield.

FIG. 5C1-5C6 are drawings showing the buildup of the plasma pinch with the blast shield in place.

FIG. 6 is a pulse shape produced by the prototype unit.

FIG. 7 shows a portion of the EUV beam produced by a hyperbolic collector.

FIG. 7A is a prospective drawing of a hyperbolic collector.

FIG. 7B shows a portion of the EUV beam produced by an ellipsoidal collector.

FIG. 8 shows the 13.5 nm lithium peak relative to reflectivity of MoSi coatings.

FIG. 9 shows a nested conical debris collector.

FIG. 10 shows thin Be window for reflecting visible light and transmitting EUV light.

FIG. 11 is a chart showing reflectivity of various materials for 13.5 mn ultraviolet radiation.

FIG. 12 is a drawing showing a technique for introducing source gas and working gas.

FIG. 13 is a time chart showing the anode voltage and EUV intensity.

FIGS. 14A, 14B, 14C and 14D show the effect of various anode designs on the plasma pinch.

FIG. 15 is a drawing showing a technique for using RF energy to operate lithium vapor source gas.

FIGS. 16, 16A, 16B, 16C, 16D and 16E show features and test results of a fourth generation prototype plasma pinch device.

FIG. 17 shows a heat pipe cooling technique for the anode in a preferred DPF device.

DETAILED DESCRIPTION OF PREFERRED EMBODIMENTS

Basic Design

Simplified drawings showing the basic design of a high energy ultraviolet light source are shown in FIGS. 1 and 1A. The major components are a plasma pinch unit 2, a high energy photon collector 4 and a hollow light pipe 6. The plasma pinch source comprises a coaxial electrode 8 powered by a low inductance pulse power circuit 10. The pulse power circuit in this preferred embodiment is a high voltage, energy efficient circuit capable of providing very fast (approximately 50 ns) rise time pulses in the range of 1.4 kV to 2.5 kV to coaxial electrode 8 at a rate of at least 1,000 Hz.

In the FIG. 1 case, a small amount of working gas, such as a mixture of helium and lithium vapor, is present near the base of the electrode 8 as shown in FIG. 1. At each high voltage pulse, avalanche breakdown occurs between the inner and outer electrodes of coaxial electrode 8 either due to preionization or self breakdown. The avalanche process occurring in the buffer gas ionizes the gas and creates a conducting plasma between the electrodes at the base of the electrodes. Once a conducting plasma exists, current flows between the inner and outer electrodes. In this preferred embodiment, the inner electrode is at high positive voltage and outer electrode is at ground potential. Current will flow from the inner electrode to the outer electrode and thus electrons will flow toward the center and positive ions will flow away from the center. This current flow generates a magnetic field which acts upon the moving charge carriers accelerating them away from the base of the coaxial electrode 8.

When the plasma reaches the end of the center electrode, the electrical and magnetic forces on the plasma, pinch the plasma to a "focus" around a point 11 along the centerline of and a short distance from the end of the central electrode and the pressure and temperature of the plasma rise rapidly reaching extremely high temperatures, in come cases much higher than the temperature at the surface of the sun! The dimensions of the electrodes and the total electrical energy in the circuit are preferably optimized to produce the desired black body temperature in the plasma. For the production of radiation in the 13 nm range a black body temperature of over 20-100 eV is required. In general, for a particular coaxial configuration, temperature will increase with increasing voltage of the electrical pulse. The shape of the radiation spot is somewhat irregular in the axial direction and roughly gausian in the radial direction. The typical radial dimension of the source is 300 microns and its length is approximately 4 mm.

In most prior art plasma pinch units described in the technical literature, the radiation spot emits radiation in all directions with a spectrum closely approximating a black body. The purpose of the lithium in the working gas is to narrow the spectrum of the radiation from the radiation spot.

A second basic design is shown in FIG. 1A. In this case, lithium vapor is the active gas and is injected through the center of the anode. The buffer gas is helium and it is

injected at a separate location. A suction pump is used to create the desired vacuum in the chamber. The lithium lines are heated to keep the lithium in a vapor state.

Lithium Vapor

Doubly ionized lithium exhibits an electronic transition at 13.5 nm and serves as the radiation source atom in the buffer of helium. Doubly ionized lithium is an excellent choice for two reasons. The first is the low melting point and high vapor pressure of lithium. The lithium ejected from the radiation spot can be kept from plating out onto the chamber walls and collection optics by simply heating these surfaces above 180°C. The vapor phase lithium can then be pumped from the chamber along with the helium buffer gas using standard turbo-molecular pumping technology. And the lithium can be easily separated from the helium merely by cooling the two gases.

Coating materials are available for providing good reflection at 13.5 nm. FIG. 8 shows the lithium emission peak in relation to the published MoSi reflectivity.

A third advantage of using lithium as the source atom is that non-ionized lithium has a low absorption cross section for 13.5 nm radiation. Furthermore, any ionized lithium ejected from the radiation spot can be easily swept away with a moderate electric field. The remaining non-ionized lithium is substantially transparent to 13.5 nm radiation. The currently most popular proposed source in the range of 13 nm makes use of a laser ablated frozen jet of xenon. Such a system must capture virtually all of the ejected xenon before the next pulse because the absorption cross section for xenon at 13 nm is large.

Xenon Broad Band Emission

Another preferred source atom is Xenon which has a broad band emission line in the range of 13.5 nm. Applicants describe in a subsequent section of this specification solutions to the absorption problem.

Radiation Collector

The radiation produced at the radiation spot is emitted uniformly into a full 4π steradians. Some type of collection optics is needed to capture this radiation and direct

it toward the lithography tool. Previously proposed 13nm light sources suggested collection optics based on the use of multi-layer dielectric coated mirrors. The use of multi-layer dielectric mirrors is used to achieve high collection efficiency over a large angular range. Any radiation source which produced debris would coat these dielectric mirrors and degrade their reflectivity, and thus reduce the collected output from the source. This preferred system will suffer from electrode erosion and thus would, over time, degrade any dielectric mirror placed in proximity to the radiation spot.

Several materials are available with high reflectivity at small grazing incident angles for 13.5 nm UV light. Graphs for some of these are shown in FIG. 11. Good choices include molybdenum, rhodium and tungsten. The collector may be fabricated from these materials, but preferably they are applied as a coating on a substrate structural material such as nickel. This conic section can be prepared by electroplating nickel on a removable mandrel.

To produce a collector capable of accepting a large cone angle, several conical sections can be nested inside each other. Each conical section may employ more than one reflection of the radiation to redirect its section of the radiation cone in the desired direction. Designing the collection for operation nearest to grazing incidence will produce a collector most tolerant to deposition of eroded electrode material. The grazing incidence reflectivity of mirrors such as this depends strongly on the mirror's surface roughness. The dependence on surface roughness decreases as the incident angle approaches grazing incidence. We estimate that we can collect and direct the 13nm radiation being emitted over a solid angle of least 25 degrees. Preferred collectors for directing radiation into light pipes are shown in FIGS. 1, 2 and 3.

Tungsten Electrodes - Tungsten Coatings for Collector

A preferred method for choosing the material for the external reflection collector is that the coating material on the collector be the same as the electrode material. Tungsten is a promising candidate since it has demonstrated performance as an electrode and the real part of its refractive index at 13nm is 0.945. Using the same material for the electrode and the mirror coating minimizes the degradation of mirror reflectivity as the eroded electrode material plates out onto the collection mirrors.

Silver Electrodes and Coatings

Silver is also an excellent choice for the electrodes and the coatings because it also has a low refractive index at 13 nm and has high thermal conductivity allowing higher repetition rate operation.

Conical Nested Debris Collector

In another preferred embodiment the collector-director is protected from surface contamination with vaporized electrode material by a debris collector which collects all of the tungsten vapor before it can reach the collector director 4. FIG. 9 shows a conical nested debris collector 5 for collecting debris resulting from the plasma pinch. Debris collector 5 is comprised of nested conical sections having surfaces aligned with light rays extending out from the center of the pinch site and directed toward the collector-director 4.

The debris collected includes vaporized tungsten from the tungsten electrodes and vaporized lithium. The debris collector is attached to or is a part of radiation collector-director 4. Both collectors are comprised of nickel plated substrates. The radiation collector-director portion 4 is coated with molybdenum or rhodium for very high reflectivity. Preferably both collectors are heated to about 400°C which is substantially above the melting point of lithium and substantially below the melting point of tungsten. The vapors of both lithium and tungsten will collect on the surfaces of the debris collector 5 but lithium will vaporize off and to the extent the lithium collects on collector-director 4, it will soon thereafter also vaporize off. The tungsten once collected on debris collector 5 will remain there permanently.

FIG. 7 shows the optical features of a collector designed by Applicants. The collector is comprised of five nested grazing incident parabolic reflectors, but only three of the five reflections are shown in the drawing. The two inner reflectors are not shown. In this design the collection angle is about 0.4 steradians. As discussed below the collector surface is coated and is heated to prevent deposition of lithium. This design produces a parallel beam. Other preferred designs such as that shown in FIGS. 1, 3 and 10 would focus the beam. The collector should be coated with a material possessing high grazing

incidence reflectivity in the 13.5 nm wavelength range. Two such materials are palladium and ruthenium.

Another collector-director designed to focus the beam is shown in FIG. 7B. This collector-director utilizes an ellipsoidal mirror 30 to focus the EUV source. Mirrors of this type are available commercially from suppliers such as Reflex S.V.O. with facilities in the Czech Republic and are distributed in the United States by Bede Scientific Instruments Ltd. with offices in the United Kingdom and Englewood, Colorado. The reader should note that this mirror collects only rays at angles shown at 32 in FIG. 7B. However, additional mirror elements could be included inside mirror 30 and outside mirror 30 to collect and focus additional rays. The reader should also note that other mirror elements could be localized downstream of mirror 30 to collect the narrow angle rays or upstream of mirror 30 to collect the wider angle rays.

Light Pipe

It is important to keep deposition materials away from the illumination optics of the lithography tool. Therefore, a light pipe 6 is preferred to further assure this separation. The lightpipe 6 is a hollow lightpipe which also employs substantially total external reflection on its inside surfaces. The primary collection optic can be designed to reduce the cone angle of the collected radiation to match the acceptance angle of the hollow lightpipe. This concept is shown in FIG. 1.

The dielectric mirrors of the lithography tool would then be very well protected from any electrode debris since a tungsten, silver or lithium atom would have to diffuse upstream against a flow of buffer gas down the hollow lightpipe as shown in FIG. 1.

Pulse Power Unit

The preferred pulse power unit 10 is a solid state high frequency, high voltage pulse power unit utilizing a solid state trigger and a magnetic switch circuit such as the pulse power units described in United States Patent 5,936,988. These units are extremely reliable and can operate continuously without substantial maintenance for many months and billions of pulses. The teachings of U.S. Patent 5,936,988 are incorporated herein by reference.

FIG. 4 shows a simplified electrical circuit providing pulse power. A preferred embodiment includes DC power supply 40 which is a command resonant charging supply of the type used in excimer lasers. C_o which is a bank of off the shelf capacitors having a combined capacitance of 65 μF, a peaking capacitor C_1 which is also a bank of off the shelf capacitors having a combined capacitance of 65 μF. Saturable inductor 42 has a saturated drive inductance of about 1.5 nH. Trigger 44 is an IGBT. Diode 46 and inductor 48 creates an energy recovery circuit similar to that described in U.S. Patent No. 5,729,562 permitting reflected electrical energy from one pulse to be stored on C_o prior to the next pulse.

The System

Thus, as shown in FIG. 1, a working gas mixture of helium and lithium vapor is discharged into coaxial electrode 8. Electrical pulses from pulse power unit 10 create a dense plasma focus at 11 at sufficiently high temperatures and pressures to doubly ionize the lithium atoms in the working gas generating ultraviolet radiation at about 13.5 nm wavelength.

This light is collected in total external reflection-collector 4 and directed into hollow light pipe 6 where the light is further directed to a lithography tool (not shown). Discharge chamber 1 is maintained at a vacuum of about 4 Torr with turbo suction pump 12. Some of the helium in the working gas is separated in helium separator 14 and used to purge the lightpipe as shown in FIG. 1 at 16. The pressure of helium in the light pipe is preferably matched to the pressure requirements of the lithography tool which typically is maintained at a low pressure or vacuum. The temperature of the working gas is maintained at the desired temperature with heat exchanger 20 and the gas is cleaned with electrostatic filter 22. The gas is discharged into the coaxial electrode space as shown in FIG. 1.

Prototype Unit

A drawing of a prototype plasma pinch unit built and tested by Applicant and his fellow workers is shown in FIG. 5A. Principal elements are C_1 capacitor decks, C_o capacitor decks, IGBT switches, saturable inductor 42, vacuum vessel 3, and coaxial electrode 8.

Test Results

FIG. 6 shows a typical pulse shape measured by Applicant with the unit shown in FIG. 5A. Applicants have recorded C_1 voltage, C_1 current and intensity at 13.5 nm over an 8 microsecond period. The integrated energy in this typical pulse is about 0.8 J. The pulse width (at FWHM) is about 280 ns. The C_1 voltage prior to breakdown is a little less than 1 KV.

This prototype embodiment can be operated at a pulse rate up to 200 Hz. The measured average in-band 13.5 nm radiation at 200 Hz is 152 W in 4π steradians. Energy stability at 1 sigma is about 6%. Applicants estimate that 3.2 percent of the energy can be directed into a useful 13.5 nm beam with the collector 4 shown in FIG. 1.

Second Plasma Pinch Unit

A second plasma pinch unit is shown in FIG. 2. This unit is similar to the plasma pinch device described in United States Patent No. 4,042,848. This unit comprises two outer disk shaped electrodes 30 and 32 and an inner disk shaped electrode 36. The pinch is created from three directions as described in Patent No. 4,042,848 and as indicated in FIG. 2. The pinch starts near the circumference of the electrodes and proceeds toward the center and the radiation spot is developed along the axis of symmetry and at the center of the inner electrode as shown in FIG. 2 at 34. Radiation can be collected and directed as described with respect to the FIG. 1 embodiment. However, it is possible to capture radiation in two directions coming out of both sides of the unit as shown in FIG. 2. Also, by locating a dielectric mirror at 38, a substantial percentage of the radiation initially reflected to the left could be reflected back through the radiation spot. This should stimulate radiation toward the right side.

Third Plasma Pinch Unit

A third embodiment can be described by reference to FIG. 3. This embodiment is similar to the first preferred embodiment. In this embodiment, however, the buffer gas is argon. Helium has the desirable property that it is relatively transparent to 13 nm radiation, but it has the undesired property that it has a small atomic mass. The low atomic mass forces us to operate the system at a background pressure of 2-4 Torr. An additional drawback of the small atomic mass of He is the length of electrode required to match the acceleration distance with the timing of the electrical drive circuit.

Because He is light, the electrode must be longer than desired so that the He falls off the end of the electrode simultaneous with the peak of current flow through the drive circuit.

A heavier atom such as Ar will have a lower transmission than He for a given pressure, but because of its higher mass can produce a stable pinch at a lower pressure. The lower operating pressure of Ar more than offsets the increased absorption properties of Ar. Additionally, the length of the electrode required is reduced due to the higher atomic mass. A shorter electrode is advantageous for two reasons. The first is a resulting reduction in circuit inductance when using a shorter electrode. A lower inductance makes the drive circuit more efficient and thus reduces the required electrical pump energy. The second advantage of a shorter electrode is a reduction in the thermal conduction path length from the tip of the electrode to the base. The majority of the thermal energy imparted to the electrode occurs at the tip and the conductive cooling of the electrode occurs mainly at the base (radiative cooling also occurs). A shorter electrode leads to a smaller temperature drop down its length from the hot tip to the cool base. Both the smaller pump energy per pulse and the improved cooling path allow the system to operate at a higher repetition rate. Increasing the repetition rate directly increases the average optical output power of the system. Scaling the output power by increasing repetition rate, as opposed to increasing the energy per pulse, is the most desired method for the average output power of lithography light sources.

In this preferred embodiment the lithium is not injected into the chamber in gaseous form as in the first and second embodiments. Instead solid lithium is placed in a hole in the center of the central electrode as shown in FIG. 3. The heat from the electrode then brings the lithium up to its evaporation temperature. By adjusting the height of the lithium relative to the hot tip of the electrode one can control the partial pressure of lithium near the tip of the electrode. One preferred method of doing this is shown in FIG. 3. A mechanism is provided for adjusting the tip of the solid lithium rod relative to the tip of the electrode. Preferably the system is arranged vertically so that the open side of coaxial electrodes 8 is the top so that any melted lithium will merely puddle near the top of the center electrode. The beam will exit straight up in a vertical direction as

indicated in FIG. 5A. (An alternative approach is to heat the electrode to a temperature in excess of the lithium melting point so that the lithium is added as a liquid.) Extremely low flow pumps are available for pumping the liquid at rates needed for any specified repetition rates. A tungsten wick can be used to wick the liquid lithium to region of the central electrode tip.

The hole down the center of the electrode provides another important advantage. Since the plasma pinch forms near the center of the tip of the central electrode, much of the energy is dissipated in this region. Electrode material near this point will be ablated and eventually end up of other surfaces inside the pressure vessel. Employing an electrode with a central hole greatly reduces the available erosion material. In addition, Applicants' experiments have shown that the existence of lithium vapor in this region further reduces the erosion rate of electrode material. A bellows or other appropriate sealing method should be used to maintain a good seal where the electrode equipment enters the chamber. Replacement electrodes fully loaded with the solid lithium can be easily and cheaply manufactured and easily replaced in the chamber.

Small Vacuum Chamber Window

The pinch produces a very large amount of visible light which needs to be separated from the EUV light. Also, a window is desirable to provide additional assurance that lithography optics are not contaminated with lithium or tungsten. The extreme ultraviolet beam produced by the present invention is highly absorbed in solid matter. Therefore providing a window for the beam is a challenge. Applicants preferred window solution is to utilize an extremely thin foil which will transmit EUV and reflect visible. Applicants preferred window is a foil (about 0.2 to 0.5 micron) of beryllium tilted at an incident angle of about 10° with the axis of the incoming beam. With this arrangement, almost all of the visible light is reflected and about 50 to 80 percent of the EUV is transmitted. Such a thin window, of course, is not very strong. Therefore, Applicants use a very small diameter window and the beam is focused through the small window. Preferably the diameter of the thin beryllium window is about 10 mm. Heating of the little window must be considered, and for high repetition rates special cooling of the window will be needed.

In some designs this element can be designed merely as a beam splitter which will simplify the design since there will be no pressure differential across the thin optical element.

FIG. 10 shows a preferred embodiment in which radiation collector 4 is extended by collector extension 4A to focus the beam 9 through 0.5 micron thick 1 mm diameter beryllium window 7.

Preionization

Applicants' experiments have shown that good results can be obtained without preionization but performance is improved with preionization. The prototype unit shown in FIG. 5A comprises DC driven spark gap preionizers to preionize the gas between the electrodes. Applicants will be able to greatly improve these energy stability values and improve other performance parameters with improved preionization techniques. Preionization is a well developed technique used by Applicants and others to improve performance in excimer lasers. Preferred preionization techniques include:

1) DC drive spark gap
2) RF driven spark gap
3) RF driven surface discharge
4) Corona discharge
5) Spiker circuit in combination with preionization

These techniques are well described in scientific literature relating to excimer lasers and are well known.

Blast Shield

FIG. 5B shows the location of two of a total of eight spark plugs 138 providing preionization in a preferred embodiment. This figure also shows the cathode 111 and the anode 123 comprised of a stainless steel outer part and a tungsten inner part. Insulator shroud encircles the lower portion of anode 123 and a 5 mill thick film insulator 125 completes the isolation of the anode from the cathode. FIGS. 5B1-6 show the progression of a typical pulse leading to a pinch which is fully developed in FIG. 5B5 at about 1.2 μs after the initiation of the discharge.

During the discharge plasma is accelerated toward the tip of the anode by the Lorentz forces acting on the ions and electrons created by the current flow through the plasma. Upon reaching the tip of the electrode shown at 121 in FIG. 5B force vectors directed radially compress and heat the plasma to high temperatures.

Once the plasma is compressed, the existing axially directed forces acting on the plasma tend to elongate the plasma column as shown especially in FIG. 5B6. It is this elongation that leads to instabilities. Once the plasma column has grown along the axis beyond a certain point, the voltage drop across the region of compressed plasma becomes too large to be sustained by the low pressure gas in the region around and near the tip of the anode. Arc-over occurs and much or all of the current flows through the shorter, lower density region of gas near the tip of the anode as shown by the dashed line in FIG. 5B6. This arc-over is detrimental because it produces instabilities in the pulse and causes relatively rapid electrode erosion.

A solution to this problem is to provide a physical barrier to motion of the plasma column in the axial direction. Such a barrier is shown as element number 143 in FIG. 5C and is called by Applicants a blast shield because it acts like a shield against the plasma exhaust of the DPF device. The blast shield must be made of an electrically insulating material with robust mechanical and thermal properties. In addition, the chemical compatibility of the blast shield material must be considered when operating with highly reactive elements such as Lithium. Lithium is a proposed emission element for this EUV source due to its intense emission at 13.5 nm. An excellent candidate is single crystal aluminum oxide, sapphire or an amorphous sapphire such as the trademarked material Lucalux manufactured by General Electric.

The optimum shape of the blast shield has been found to be a dome centered on the anode with a radius equal to the diameter of the anode as shown in FIG. 5C. Such a shape closely matches the naturally occurring plasma current lines when the plasma is under maximum compression. If the blast shield is placed further from the anode tip, then the plasma column will be too long leading to insufficient plasma heating and the risk of arc-over. If the blast shield is placed too close to the anode tip then current flow

from the central axis out and down toward the cathode is restricted, again leading to insufficient plasma heating.

The hole in the top side of blast shield 143 at 144 is required to allow EUV radiation to escape and be collected for use. This hole must be made as small as possible due to the tendency of the plasma to leak out through this hole and form a long narrow column above the blast shield. A bevel cut into this hole as shown at 144 allows for greater off-axis collection of the EUV radiation produced by the plasma pinch device.

FIGS. 5C1-6 show how the blast shield contains the plasma pinch and prevents arc-over.

Combination of Gas Types and Densities

Applicants have discovered that the requirements of the source gas and that of an optimized buffer gas are not satisfied by a single gas. The source gas must be something like Lithium for narrow-band emission at 13.5 nm or Xenon for broad-band emission near 13.5 nm. The density, break-down and absorption properties of Lithium and Xenon are not optimum for use as a buffer gas. For example, Xenon is too strongly self-absorbing and Lithium is not sufficiently dense for use as a buffer gas.

To address this problem of conflicting requirements, Applicants as shown in FIG. 12 separate the working gas into a source gas and a buffer gas and provide a source gas feed 42 such as a mixture of 5% Xe and 95% He up the center of the anode 40. Applicants then provide an optimized buffer gas such as helium or a mixture of helium and argon to the main vessel region maintained at a constant pressure. The source gas inside the anode will then be at the pressure of the buffer gas and the flow rate of source gas 42 determine the partial pressure of source gas mixed in with the buffer gas in the main vessel region. It is optimum to have a low source gas flow rate to minimize the partial pressure of the source gas in the main vessel region. (The working gas pressure in the main vessel region is regulated by a pressure regulation system not shown.) The buffer gas is circulated between the anode 40 and cathode 44 as shown at 46.

Optimizing Capacitance

Applicants have discovered that the highest plasma temperature exists when the plasma pinch event occurs simultaneous with the peak of the current flow from the drive capacitor bank. For a given anode configuration and buffer gas density, the plasma front will travel down the length of the anode in a given amount of time for a given amount of charge voltage. Maximum emission efficiency is obtained by adjusting the capacitance value and charge voltage such that the peak capacitor current exists during the plasma pinch event.

If a higher input energy level is desired and thus a higher charge voltage, then the drive capacitance must be reduced so that the timing of the drive waveshape matches the plasma run down time along the length of the anode. Since energy stored on a capacitor scales as the square of voltage and linearly with capacitance, the stored energy will increase linearly with voltage as one decreases capacitance proportional with increases in voltage.

FIG. 13 is a drawing showing the measured drive capacitance voltage, the measured anode voltage and the EUV intensity versus time for a preferred embodiment with the capacitance properly chosen to produce maximum capacitor current during the pinch. In this case, for a 2 cm long anode, a He buffer gas pressure of 2.5 Torr and a C_1 capacitance of 3 μF.

Optimum Anode Shape

Applicants have discovered with hollow anode configurations, that the plasma pinch grows rapidly along the axis once the pinch has been formed, and will extend down the opening in the hollow anode. As this pinch grows in length, it eventually drops too much voltage along its length and an arc-over occurs across the surface of the anode. One solution to prevent this arc-over makes use of a blast shield to provide a physical barrier to the growth of the pinch length extending away from the anode as described above. Another solution to reduce the rate of pinch length growth down into the hollow anode is to increase the open diameter inside the anode narrow region. This will slow the growth of the pinch length and prevent arc-over.

All previous literature shows a hollow anode with a constant dimension hollow portion.

FIGS. 14A, 14B, 14C and 14D show examples of pinch shapes for various hollow anode shapes. The configuration shown in FIG. 14D shows the shortest pinch shape.

Exposed Anode Length

Since the plasma run down time determines where on the drive voltage waveshape the pinch occurs, Applicants have been able to adjust the duration of the pinch portion of the plasma focus device by changing the amount of exposed anode and thus the duration of the rundown.

The buffer gas density is dictated by a desired plasma pinch diameter, and the drive capacitance is in practice limited to within a certain range. These two parameters, combined with the drive voltage determine the desired run down time. The run down time can then be adjusted by increasing or decreasing the length of exposed anode. Preferably, the run down time is chosen such that the plasma pinch event occurs during the peak in the drive current waveshape. If a longer plasma pinch duration is desired then the exposed length of the anode can be reduced, thus shortening the run down time and causing the plasma pinch to occur earlier in the drive waveshape.

Lithium Delivery Technique

Lithium delivery schemes described above depend on raising the anode temperature sufficiently high that the vapor pressure of Lithium reached a desired level. Such temperatures are in the range of 1000 – 1300°C.

An alternative is to fabricate an RF antenna from a material such as porous Tungsten impregnated with Lithium. This porous Lithium filled Tungsten antenna 50 is placed down inside the anode as shown in FIG. 15. RF power source 52 creates a plasma-layer on and near the antenna will drive off atoms that are swept up by the gas flow 54 through the center of the hollow anode and the Lithium atoms carried to the end of the anode.

The rate of Lithium ion production is easily controlled by the power level of the RF source. In addition, the porous Tungsten anode can be maintained with this RF drive

at a temperature sufficient for liquid Lithium to wick up from a reservoir 56 placed at the bottom of the anode.

Anode Cooling

In preferred embodiments of the present invention the central anode has an outside diameter in the range of about 0.5 cm to 1.25 cm. The anode is expected to absorb substantial energy due to the plasma fall during discharge and due to absorption of radiation from the plasma pinch. Cooling in the range of about 15 kw may be required. Because the gas pressure is very low there cannot be much cooling due to convection through the buffer gas. Radiation cooling could only be effective at very high anode temperatures. Conduction down the anode length would require a very large temperature drop.

If lithium vapor is used as an active gas and is injected through the center of the anode the anode temperature will need to be maintained at temperatures in the range of 1,000°C to 1,300°C or higher. This high temperature of operation, substantial heat removal requirement, envelope considerations and the high voltage limit the choices of cooling technique. One technology, however, a lithium (or other alkali metal) heat pipe, offers the potential for a relatively simple and robust solution. Lithium heat pipes begin to operate efficiently at temperatures of about 1000°C. The specific design of such devices typically use refractory metals, molybdenum and tungsten, for the casing and internal wick and can therefore operate at very high temperatures. Initial investigations reveal that there is confidence that such a heat pipe is capable of meeting the cooling requirements of the DPF.

The simplest embodiment would take the form of a tubular or annular heat pipe that is integral with the anode of the DPF for best thermal coupling. A likely embodiment would be annular to enable the delivery of liquid or vaporized lithium to the plasma of the DPF. By way of an example a .5" diameter solid heat pipe removing 15 kW would have a watt density of 75kW/in^2 (11.8 kW/cm^2). An annular heat pipe having an OD of 1" and an ID of .5" removing 15 kW of heat would have a watt density of 25.4 kW/in^2 (3.9 kW/cm^2). Both of these examples illustrate the potential of this technology since watt densities far in excess of 15 kW/cm^2 have been demonstrated with lithium

heat pipes. In operation, heat pipes have only a very small temperature gradient along their length and can be considered as having constant temperature with length for practical purposes. Therefore the "cold" (condenser) end of the heat pipe will also be at some temperature at or above 1000°C. To remove heat from the condenser end of the heat pipe a preferred embodiment may utilize radiative cooling to a liquid coolant (such as water) jacket. Radiative heat transfer scales as the fourth power of temperature, therefore, high rates of heat transfer will be possible at the proposed operating temperatures. The heat pipe would be surrounded by an annular water heat exchanger capable of steady state operation at 15 kW. Other embodiments may insulate the condenser end of the heat pipe with another material such as stainless steel and cool the outer surface of that material with a liquid coolant. Whatever technique is used, it is important that the heat pipe is not "shocked" with a coolant at the condenser, i.e., forced to be much cooler than the evaporator end. This can seriously impact performance. Also if the heat pipe temperature falls below the freezing temperature of the working fluid at any point along its length (~180°C for lithium) it will not work at all.

Restrictions to the operating temperature of components near the base of the central electrode (anode) may require that heat transferred to this region be minimized. This condition may be accomplished, for example, by coating the exterior of the heat pipe with a low emissivity material near the region of lower temperature tolerance. A vacuum gap can then be fabricated between the heat pipe and the desired lower temperature components. Since vacuum has very low thermal conductivity and the heat pipe is coated with a low emissivity material, minimal heat transfer will occur between the heat pipe and the cooler components. Maintaining a controlled anode temperature under varying power load levels is another consideration. This may be accomplished by placing a cylinder between the heat pipe and the water cooled outer jacket. This cylinder would be coated or finished for high reflectivity on its inner diameter and for low emissivity on its outer diameter. If the cylinder is fully inserted between the radiating heat pipe and the water cooling jacket, radiation will be reflected back toward the heat pipe thus reducing the power flow from heat pipe to jacket. As the "restrictor" cylinder is extracted a greater proportion of the heat pipe's condenser can radiate directly onto the water jacket heat exchanger. Adjustment of the "restrictor" position

thus controls the power flow which sets the steady state operating temperature of the heat pipe, and ultimately the anode.

A preferred embodiment using heat pipe cooling is shown in FIG. 17 shown in the drawing are anode 8A, cathode 8B, and insulator element 9. In this case, lithium vapor is used as the active gas and is delivered into the discharge chamber through the center of anode 8A as shown at 440. Anode 8A is cooled with lithium heat pipe system 442 comprising lithium heat pipe 444. Lithium within the heat transfer region 446 of heat pipe 444 vaporizes near the hot end of the electrode 8A and the vapor flows toward the cooler end of the heat pipe where heat is transferred from the heat pipe by radiative cooling to a heat sink unit 446 having a heat sink surface 448 cooled by water coil 450. The cooling of the lithium vapor causes a change in its state to liquid and the liquid is wicked back to the hot end by capillary pumping in accordance with well known heat pipe technology. In the embodiment a restrictor cylinder 452 slides up and down as shown at 454 inside heat sink surface 448 based on a drive which is part of a temperature feedback control unit not shown. The anode heat pipe unit also preferably comprises an auxiliary heating system for maintaining the lithium at temperatures in excess of its freezing point when the plasma pinch device is not producing sufficient heat.

Fourth Generation Device

FIG. 16 is a cross section drawing of a fourth generation prototype plasma pinch device 400 built and tests by Applicants. FIG. 16A is an enlarged portion of the device showing in greater detail the pinch region 401. FIG. 16B is a circuit diagram showing the important electrical elements of the high voltage pulse power drive system for this embodiment. This unit produces plasma pinches at pulse repetition rates of up to about 2 kHz. The electrical energy discharged between the electrodes is about 12 J per pulse. Applicants estimate that the useful light energy produced by each pinch in the EUV range of interest is radiated into 2 π steradians is in the range of about 20 mJ.

Substantially all of the components shown in FIG. 16 area part of the solid state pulse power system 404 for supplying the discharge electrical pulses of the electrodes. In this embodiment, a positive voltage pulse of about 4-5 kv is applied to the central anode 8A.

The cathode 8B is at ground potential. Preionization is provided by 8 spark plugs 138 which produce preionization sparks at the bottom of the space between the cathode and the anode. These spark plugs operate at 20 kv using as a power supply a 30 kv 10 mHz sine wave generator (not shown).

Electrical Circuit

A description of the electrical circuit diagram of this preferred pulse power system is set forth below with reference to FIG. 16B and occasionally to FIGS. 16 and 16A.

Plasma Focus Power System

A conventional approximately 700 V dc power supply is used to convert ac electrical power from utility 208 volt, 3 phase power into approximately 700 V dc 50 A power. This power supply 400 provides power for resonant charger unit 402. Power supply 400 charges up a large 1500 μF filter capacitor bank, C-1. Upon command from the external trigger signal, the resonant charger initiates a charging cycle by closing the command-charging switch, S1. Once the switch closes, a resonant circuit is formed from the C-1 capacitor, a charging inductor L1, and a C0 capacitor bank which forms a part of solid pulse power system (SSPPS) 404. Current therefore begins to discharge from C-1 through the L1 inductor and into C0, charging up that capacitance. Because the C-1 capacitance is much, much larger than the C0 capacitance, the voltage on C0 can achieve approximately 2 times the initial voltage of that on C-1 during this resonant charging process. The charging current pulse assumes a half-sinusoidal shape and the voltage on C0 resembles a "1-cosine" waveform.

In order to control the end voltage on C0, several actions may take place. First, the command-charging switch S1 can be opened up at any time during the normal charging cycle. In this case, current ceases to flow from C-1 but the current that has already been built up in the charging inductor continues to flow into C0 through the free-wheeling diode D3. This has the effect of stopping any further energy from C-1 from transferring to C0. Only that energy left in the charging inductor L1 (which can be substantial) continues to transfer to C0 and charge it to a higher voltage.

In addition, the de-qing switch S2 across the charging inductor can be closed, effectively short-circuiting the charging inductor and "de-qing" the resonant circuit. This essentially removes the inductor from the resonant circuit and prevents any further current in the inductor from continuing to charge up C0. Current in the inductor is then shunted away from the load and trapped in the loop made up of charging inductor L1, the de-qing switch S2, and the de-qing diode D4. Diode D4 is included in the circuit since the IGBT has a reverse anti-parallel diode included in the device that would normally conduct reverse current. As a result, diode D4 blocks this reverse current which might otherwise bypass the charging inductor during the charging cycle.

Finally, a "bleed down" or shunt switch and series resistor (both not shown in this preferred embodiment) can be used to discharge energy from C0 once the charging cycle is completely finished in order to achieve very fine regulation of the voltage on C0.

The dc power supply is a 208 V, 90 A, ac input, 800 V, 50 A dc output regulated voltage power supply provided by vendors such as Universal Voltronics, Lambda/EMI, Kaiser Systems, Sorensen, etc. A second embodiment can use multiple, lower power, power supplies connected in series and/or parallel combinations in order to provide the total voltage, current, and average power requirements for the system.

The C-l capacitor is comprised of two 450 V dc, 3100 μF, electrolytic capacitors connected together in series. The resulting capacitance is 1500 μF rated at 900 V, providing sufficient margin over the typical 700-800 V operating range. These capacitors can be obtained from vendors such as Sprague, Mallory, Aerovox, etc.

The command charging switch S1 and output series switch S3 in the embodiment are 1200 V, 300 A IGBT switches. The actual part number of the switches is CM300HA-24H from Powerex. The de-qing switch S2 is a 1700 V, 400 A IGBT switch, also from Powerex, part number CM400HA-34H.

The charging inductor L1 is a custom made inductor made with 2 sets of parallel windings (20 turns each) of Litz wire made on a toroidal, 50-50% NiFe tape wound core with two 1/8" air gaps and a resulting inductance of approximately 140 μH . National

Arnold provides the specific core. Other embodiments can utilize different magnetic materials for the core including Molypermaloy, Metglas™, etc.

The series, de-qing, and freewheeling diodes are all 1400 V, 300 A diodes from Powerex, part number R6221430PS.

As mentioned above, the SSPPS is similar to those referred to above as being described in the prior art. Once the resonant charger 402 charges up C0, a trigger is generated by a control unit (not shown) in the resonant charges that triggers the IGBT switches S4 to close. Although only one is shown in the schematic diagram (for clarity), S4 consists of eight parallel IGBT's which are used to discharge C0 into C1. Current from the C0 capacitors then discharges through the IGBT's and into a first magnetic switch LS1. Sufficient volt-seconds are provided in the design of this magnetic switch to allow all of the 8 parallel IGBT's to fully turn on (i.e. close) prior to substantial current building up in the discharge circuit. After closure the main current pulse is generated and used to transfer the energy from C0 into C1. The transfer time from C0 to C1 is typically on the order of 5 μs with the saturated inductance of LS1 being approximately 230 nH. As the voltage on C1 builds up to the full desired voltage, the volt-seconds on a second magnetic switch LS2 run out and that switch saturates, transferring the energy on C1 into 1:4 pulse transformer 406 which is described in more detail below. The transformer basically consists of three one turn primary "windings" connected in parallel and a single secondary "winding". The secondary conductor is tied to the high voltage terminal of the primaries with the result that the step-up ratio becomes 1:4 instead of 1:3 in an auto-transformer configuration. The secondary "winding" is then tied to C2 capacitor bank that is then charged up by the transfer of energy from C1 (through the pulse transformer). The transfer time from C1 to C2 is approximately 500 ns with the saturated inductance of LS2 being approximately 2.3 nH. As the voltage builds up on C2, the volt-second product of the third magnetic switch LS3 is achieved and it also saturates, transferring the voltage on C2 to anode 8a as shown on FIGS. 14A and 14B. The saturated inductance of LS3 is approximately 1.5 nH.

A fourth magnetic switch is provided as a protection device in case the DPF is not functioning properly. In the case where the pre-ionization pulse is not applied at the

right time (just prior to the main pulse), the main pulse voltage is not sufficient to break down the insulator between the anode and cathode. As a result, the pulsed voltage into this open-circuit condition can essentially double leading to an undesirable breakdown in the machine at some location other than the desired DPF electrodes. In this case, most of the energy is then reflected back to the "front end" of the SSPPS. Such a large reverse voltage pulse can cause avalanching of the series diode in the SSPPS, leading to potential damage or destruction of the devices. This fourth magnetic switch is designed such that volt-second product will be exceeded if the main DPF electrodes do not break down. In this instance, the magnetic switch is designed to short the load prior to the voltage doubling and causing significant damage. The saturated inductance of the fourth magnetic switch LS4 is approximately 22 nH and it is terminated into a parallel RL load with ~ 1.5 ohms resistance and ~75 μH inductance.

Bias circuitry shown in the schematic diagram 14B at 408 is also used to properly bias the four magnetic switches. Current from the bias power supply V1, passes through magnetic switches LS4 and LS3. It then splits and a portion of the current passes through bias inductor L5 and back to the bias power supply V1. The remainder of the current passes through the pulse transformer secondary winding and then through magnetic switches LS2 and LS1 and bias inductor L3 back to the bias power supply V1. Bias inductor L2 provides a path back to the power supply from current through the pulse transformer primary to ground. Bias inductors L3 and L5 also provide voltage isolation during the pulse in the SSPPS since the bias power supply Vl operates close to ground potential (as opposed to the potentials generated in the SSPPS where the bias connections are made).

The C0, C1 and C2 capacitances are made up of a number of parallel, polypropylene film capacitors mounted on a printed circuit board with thick (6-10 oz.) copper plating. The printed circuit boards are wedge shaped such that 4 boards make up a cylindrical capacitor deck which feeds a cylindrical bus for both the high voltage and ground connections. In such a way, a low inductance connection is formed which is important to both the pulse compression and to the stability of the plasma pinch in the DPF itself. The total capacitance for C0 and C1 are 21.6 μF each while the total capacitance for C2 is 1.33 μF. The C0 and C1 capacitors are 0.1 μF, 1600 V capacitors obtained from

vendors such as Wima in Germany or Vishay Roederstein in North Carolina. The C2 capacitance is made up of three sections of capacitors stacked in series to achieve the overall voltage rating since the voltage on the secondary of the pulse transformer is ~5 kv. The C2 capacitors are 0.01 μF, 2000 V dc components, again from Wima or Vishay Roederstein.

The SSPPS switches are 1400 V, 1000 A IGBT switches. The actual part number is CM1000HA-28H from Powerex. As noted earlier, 8 parallel IGBT switches are used to discharge C0 into C1.

The SSPPS series diodes are all 1400 V, 300 A diodes from Powerex, part number R6221430. Two diodes are used for each IGBT switch, resulting in a total of sixteen parallel devices.

Magnetic switch LS1 is a custom made inductor made with 16 sets of parallel windings (6 turns each) of Litz wire made on a toroidal, ferrite core. The specific core is provided by Ceramic Magnetics of New Jersey and is made of CN-20 ferrite material. The toroid is 0.5" thick with an I.D. of 5.0" and an O.D. of 8.0".

Magnetic switch LS2 is a single turn, toroidal inductor. The magnetic core is tape wound on a 8.875" O.D. mandrel using 2" wide, 0.7 mil thick, 2605-S3A Metglas™ from Honeywell with 0.1 mil thick Mylar wound in between layers to an outside diameter 10.94".

Magnetic switch LS3 is also a single turn, toroidal inductor. The magnetic core is tape wound on a 9.5" O.D. mandrel using 1" wide, 0.7 mil thick, 2605-S3A Metglas™ from Honeywell with 0.1 mil thick Mylar wound in between layers to an outside diameter of 10.94".

The pulse transformer is similar in construction to that described in U.S. Patent No. 5,936,988. Each of the three transformer cores is tape would on a 12.8" O.D. mandrel 422 using 1" wide, 0.7 mil thick, 2605-S3A Metglas™ from Honeywell with 0.1 mil thick Mylar wound in between layers to an outside diameter of 14.65". Each of the three cores 418 are ring shaped, 12.8 I.D. and about 14 inch O.D. having heights of 1 inch. An axial cross section sketch showing the physical arrangement of the three cores

and the primary and secondary "windings" is shown in FIG. 14C. Each of the primary windings actually are formed from two circular rings 420A and 420B bolted to mandrel 422 and rod-like spacers 424. The secondary "winding" is comprised of 48 circularly spaced bolts 426.

The transformer operates on a principal similar to that of a linear accelerator. A high voltage current pulse in the three primary "windings" induce a voltage rise in the secondary "winding" approximately equal to the primary voltage. The result is a voltage generated in the secondary winding (i.e., rods 426) equal to three times the primary voltage pulse. But since the low voltage side of the secondary winding is tied to the primary windings a four fold transformation is provided.

Bias inductors L3 and L4 are both toroidal inductors wound on a Molypermalloy magnetic core. The specific core dimensions are a height of 0.8", an I.D. of 3.094", and an O.D. of 5.218". The part number of the core is a-430026-2 from Group Arnold. Inductor l3 has 90 turns of 12 AWG wire wound on the toroid for an inductance of ~7.3 mH while L4 has 140 turns of 12 AWG wire wound on it for an inductance of ~18 mH.

Bias inductor L6 is merely 16 turns of 12 AWG wire wound in a 6" diameter. Bias inductor L4 is 30 turns of 12 AWG wire in a 6" diameter. Bias inductor L2 is 8 turns of 12 AWG wire in a 6" diameter.

Resistor R1 is an array of twenty parallel resistors, each of which is 27 ohm, 2W carbon composition resistor.

Energy Recovery

In order to improve the overall efficiency this fourth generation dense plasma focus device provides for energy recovery on a pulse-to-pulse basis of electrical pulse energy reflected from the discharge portion of the circuit. The energy recovery technique utilized herein is similar to that described in U.S. Patent No. 5,729,562 which is incorporated herein by reference. Energy recovery is achieved as explained below by reference to FIG. 16B.

After the discharge C2 is driven negative. When this occurs, LS2 is already saturated for current flow from C1 to C2. Thus, instead of having energy ringing in the device (which tends to cause electrode erosion) the saturated state of LS2 causes the reverse charge on C2 to be transferred resonantly back into C1. This transfer is accomplished by the continued forward flow of current through LS2. After the transfer of charge from C2 to C1, C1 then has a negative potential as compared to C0 (which at this time is at approximately ground potential) and (as was the case with LS2) LS1 continues to be forward conducting due to the large current flow during the pulse which has just occurred. As a consequence, current flows from C0 to C1 bringing the potential of C1 up to about ground and producing a negative potential on C0.

The reader should note that this reverse energy transfers back to C0 is possible only if all the saturable inductors (LS1, LS2 and LS3) remain forward conducting until all or substantially all the energy is recovered on C0. After the waste energy is propogated back into C0, C0 is negative with respect to its initial stored charge. At this point switch 54 is opened by the pulse power control. Inverting circuit comprising inductor L1 and solid state diode D3 coupled to ground causes a reversal of the polarity of C0 as the result of resonant free wheeling (i.e., a half cycle of ringing of the L1-C0 circuit as clamped against reversal of the current in inductor L1 by diode D3 with the net result that the energy is recovered by the partial recharging of C0. Therefore, the energy which otherwise would have contributed to the erosion of the electrodes is recovered reducing the charging requirements for the following pulse.

Test Results

FIGS. 16D and 16E show test results from the fourth generation prototype device. FIG. 16D shows the pulse shape on capacitor C2 and across the electrodes and FIG. 16E shows a measured photo diode signal with Xenon as the active gas.

It is understood that the above described embodiments are illustrative of only a few of the many possible specific embodiments which can represent applications of the principals of the present invention. For example, instead of recirculating the working

gas it may be preferable to merely trap the lithium and discharge the helium. Use of other electrode - coating combinations other than tungsten and silver are also possible. For example copper or platinum electrodes and coatings would be workable. Other techniques for generating the plasma pinch can be substituted for the specific embodiment described. Some of these other techniques are described in the patents referenced in the background section of this specification, and those descriptions are all incorporated by reference herein. Many methods of generating high frequency high voltage electrical pulses are available and can be utilized. An alternative would be to keep the lightpipe at room temperature and thus freeze out both the lithium and the tungsten as it attempts to travel down the length of the lightpipe. This freeze-out concept would further reduce the amount of debris which reached the optical components used in the lithography tool since the atoms would be permanently attached to the lightpipe walls upon impact. Deposition of electrode material onto the lithography tool optics can be prevented by designing the collector optic to re-image the radiation spot through a small orifice in the primary discharge chamber and use a differential pumping arrangement. Helium or argon can be supplied from the second chamber through the orifice into the first chamber. This scheme has been shown to be effective in preventing material deposition on the output windows of copper vapor lasers. Lithium hydride may be used in the place of lithium. The unit may also be operated as a static-fill system without the working gas flowing through the electrodes. Of course, a very wide range of repetition rates are possible from single pulses to about 5 pulses per second to several hundred or thousands of pulses per second. If desired, the adjustment mechanism for adjusting the position of the solid lithium could be modified so that the position of the tip of the central electrode is also adjustable to account for erosion of the tip.

Many other electrode arrangements are possible other than the ones described above. For example, the outside electrode could be cone shaped rather than cylindrical as shown with the larger diameter toward the pinch. Also, performance in some embodiments could be improved by allowing the inside electrode to protrude beyond the end of the outside electrode. This could be done with spark plugs or other preionizers well known in the art. Another preferred alternative is to utilize for the outer electrode an array of rods arranged to form a generally cylindrical or conical

shape. This approach helps maintain a symmetrical pinch centered along the electrode axis because of the resulting inductive ballasting.

Accordingly, the reader is requested to determine the scope of the invention by the appended claims and their legal equivalents, and not by the examples which have been given.

CLAIMS

What is claimed is:

1. A high energy photon source comprising:

A. a vacuum chamber,

B. at least two electrodes mounted coaxially within said vacuum chamber and defining an electrical discharge region and arranged to create high frequency plasma pinches at a pinch site upon electrical discharge,

C. a working gas comprising an active gas and a buffer gas, said buffer gas being a noble gas, and said active gas being chosen to provide light at least one spectral line,

D. an active gas supply system for supplying the active gas to said discharge region,

E. a pulse power system comprising a charging capacitor and a magnetic compression circuit said magnetic compression circuit comprising a pulse transformer for providing electrical pulses and voltages high enough to create electrical discharge between said at least one pair of electrode.

2. A high energy photon source as in Claim 1 wherein one of said two electrodes is a hollow anode and said active gas is introduced into said vacuum chamber through said hollow anode.

3. A high energy photon source as in Claim 2 wherein said active gas comprise lithium.

4. A high energy photon source as in Claim 3 wherein said active gas comprise Xenon.

5. A high energy photon source as in Claim 2 wherein said buffer gas is a noble gas.

6. A high energy photon source as in Claim 2 wherein said pulse power source comprises at least one capacitor optimized to provide peak capacitor current simultaneous with said plasma pinch.

7. A high energy photon source as in Claim 2 wherein said hollow anode defines a pinch end and first an inside diameter near said pinch end and a second inside diameter farther from said pinch end than said first inside diameter, wherein said second inside diameter is larger than said first inside diameter.

8. A high energy photon source as in Claim 7 wherein said first inside diameter extends from said pinch end by a distance chosen to prevent arc-over.

9. A high energy photon source as in Claim 2 wherein said anode defines an exposed anode length and said length is chosen so that a plasma pinch occurs approximately simultaneously with a peak drive current.

10. A high energy photon source as in Claim 2 and further comprising a lithium source comprised of a porous material infiltrated with lithium.

11. A high energy photon source as in Claim 10 wherein said porous material is porous tungsten.

12. A high energy photon source as in Claim 11 wherein said source further comprises an RF source configured to create a plasma surrounding at least a portion of said porous material.

13. A high energy photon source as in Claim 1 wherein said pulse power system comprises a resonance charging system for charging said charging capacitor.

14. A high energy photon source as in Claim 1 wherein said magnetic compression circuit comprising at least two saturable inductors and a bias circuit for biasing said at least two saturable inductors.

15. A high energy photon source as in Claim 1 and further comprising an energy recovery circuit for recovering on said charging capacitor energy reflected from said electrodes.

16. A high energy photon source wherein said charging capacitor is comprised of a bank of individual capacitors.

17. A high energy photon source as in Claim 1 and further comprising a heat pipe for cooling at least one of said electrodes.

18. A high energy photon source as in Claim 2 and further comprising a heat pipe cooling system for cooling said hollow anode.

19. A high energy photon source as in Claim 18 wherein said heat pipe cooling system and said hollow cathode comprise a heat pipe cooled hollow cathode having a portion for the introduction of said active gas.

20. A high energy photon source as in Claim 1 wherein said pulse transformer is comprised of a plurality of ring shaped cores comprised of magnetic material and a primary winding in electromagnetic association with each of said cores.

21. A high energy photon source as in Claim 20 wherein said magnetic material is comprised of high permability film wrapped on a mandrel.

22. A high energy photon source as in Claim 21 wherein said pulse transformer defines a secondary winding comprised of a plurality of rods.

23. A high energy photon source as in Claim 21 wherein said mandrel form a part of said primary winding for each primary winding.

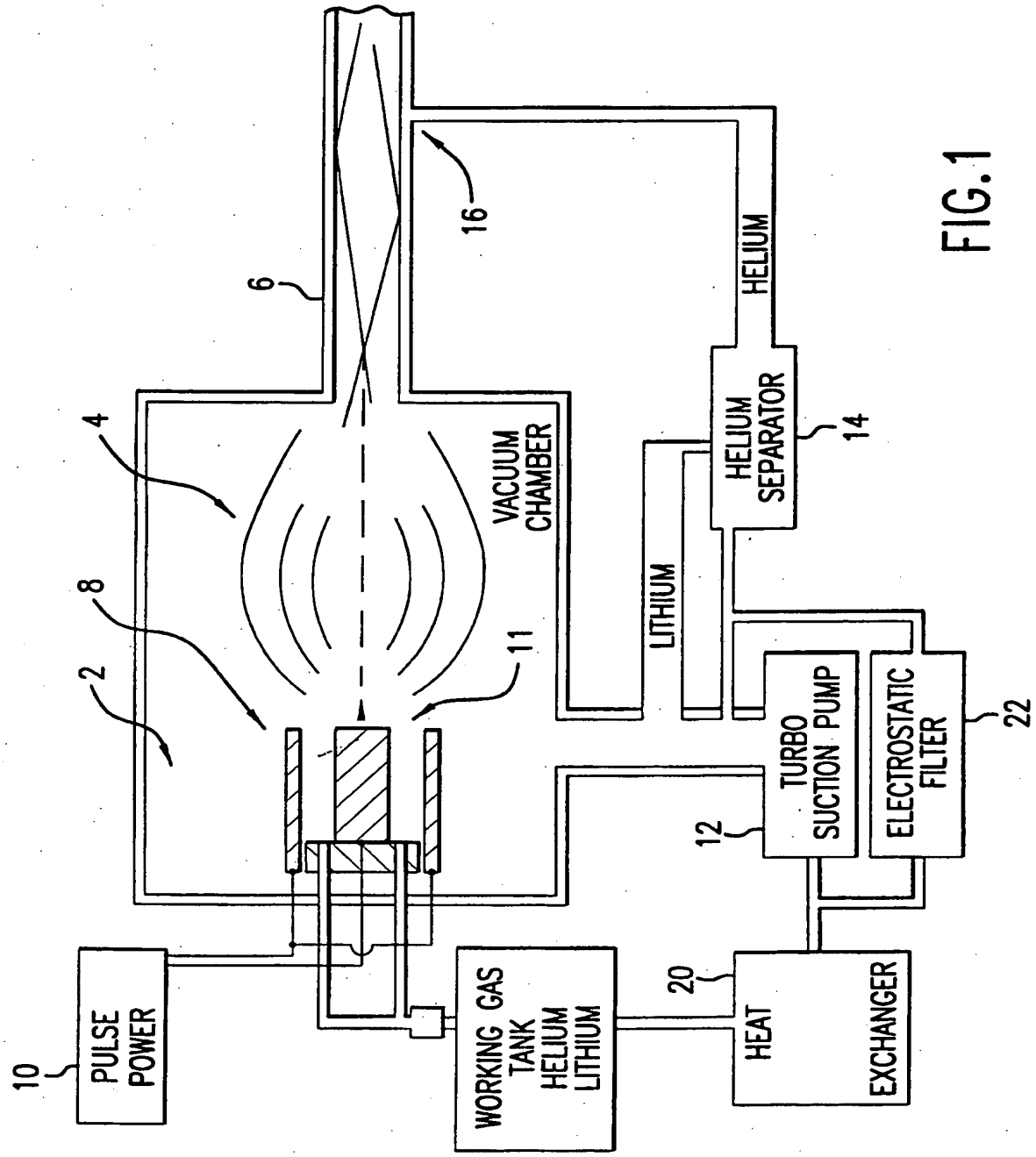
16
6
HELIUM
4
VACUUM CHAMBER
HELIUM SEPARATOR
14
8
11
LITHIUM
2
TURBO SUCTION PUMP
ELECTROSTATIC FILTER
22
12
10
PULSE POWER
WORKING GAS TANK HELIUM LITHIUM
20
HEAT EXCHANGER

FIG.1

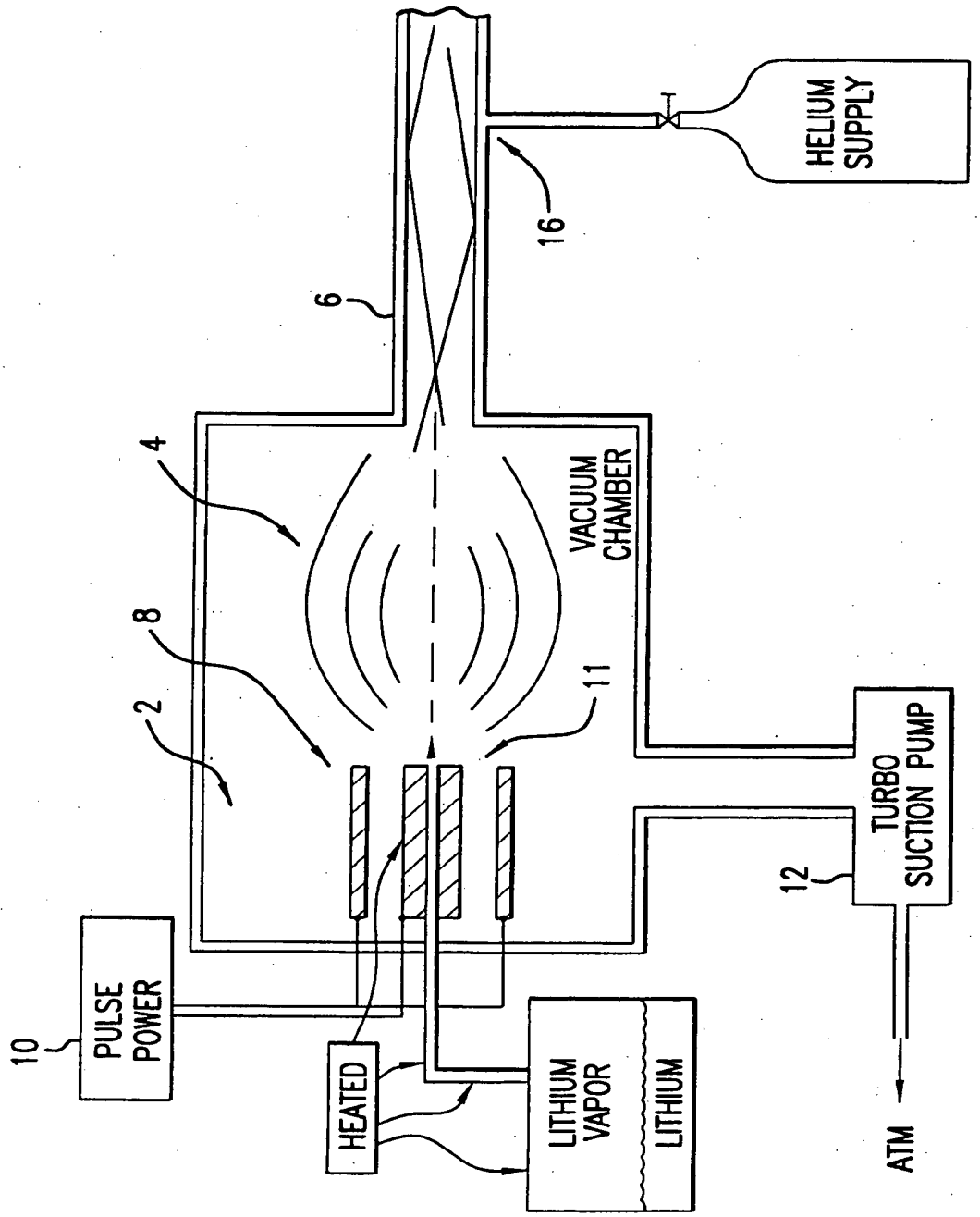
HELIUM SUPPLY
16
6
4
VACUUM CHAMBER
8
2
11
TURBO SUCTION PUMP
12
PULSE POWER
10
HEATED
LITHIUM VAPOR
LITHIUM
ATM

FIG. 1A

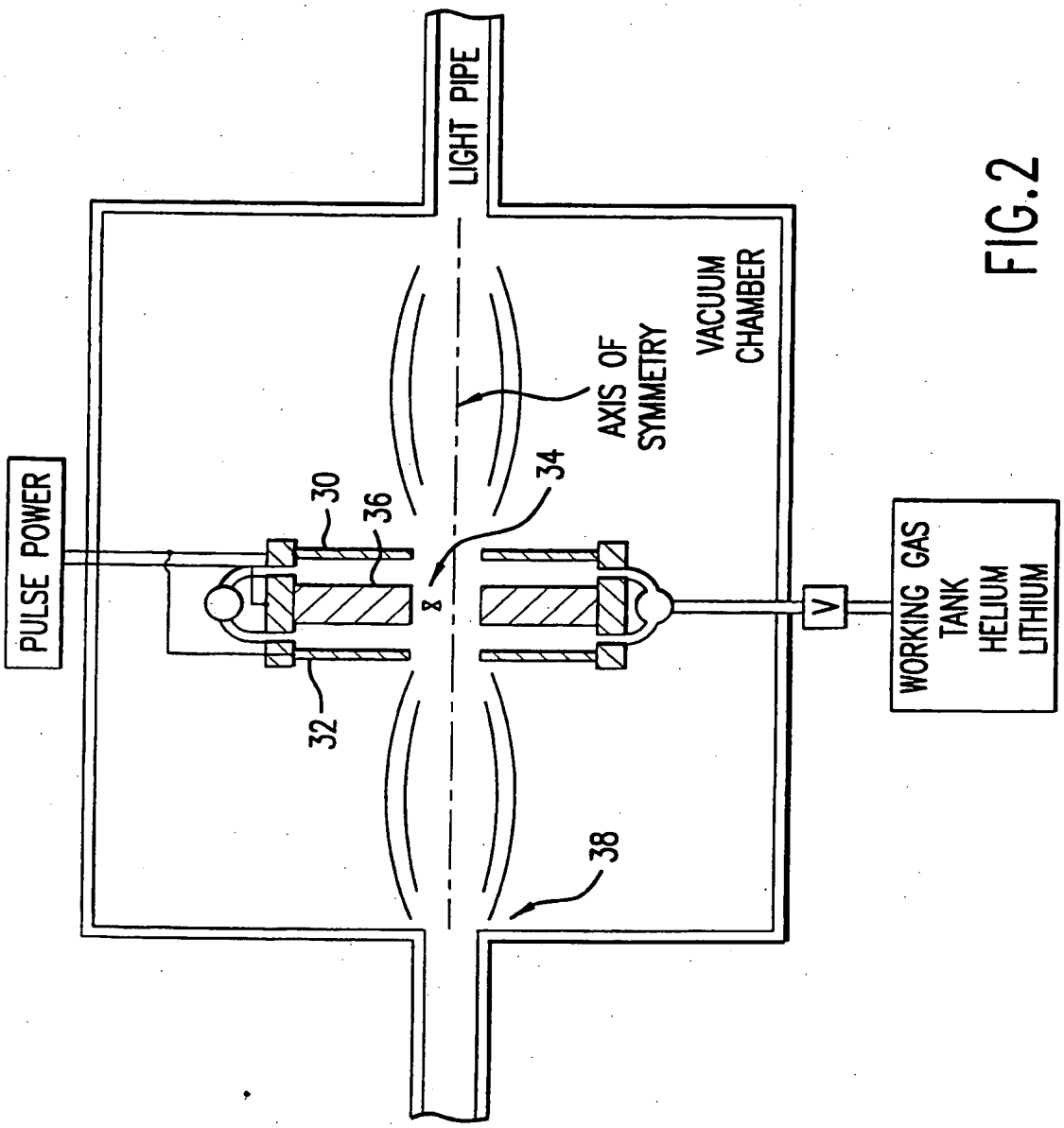
LIGHT PIPE
VACUUM CHAMBER
AXIS OF SYMMETRY
PULSE POWER
30
36
34
32
38
V
WORKING GAS TANK
HELIUM
LITHIUM

FIG.2

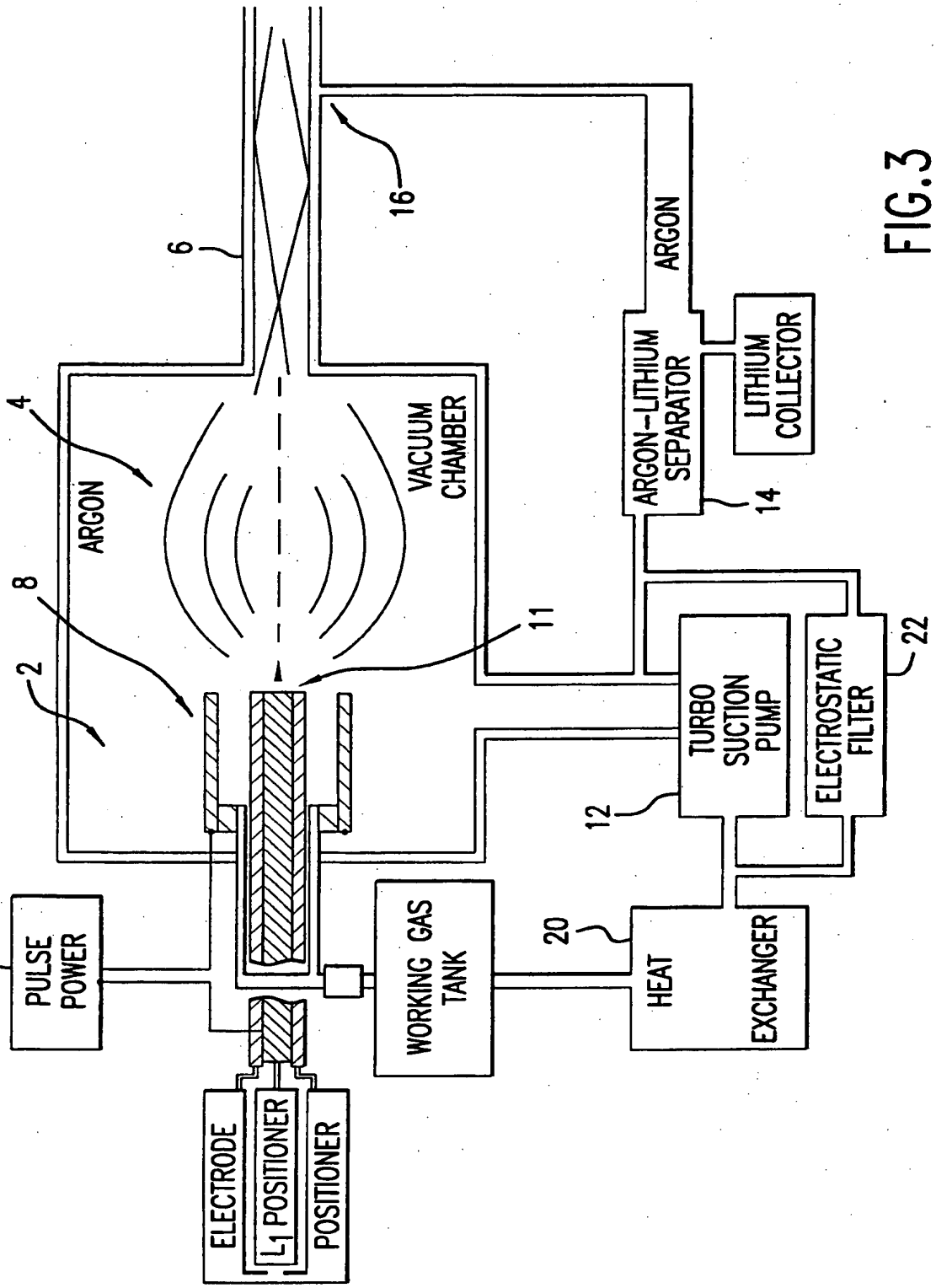
16
6
4
ARGON
8
2
VACUUM CHAMBER
11
ARGON
ARGON-LITHIUM SEPARATOR
LITHIUM COLLECTOR
14
TURBO SUCTION PUMP
ELECTROSTATIC FILTER
22
12
10
PULSE POWER
WORKING GAS TANK
20
HEAT EXCHANGER
ELECTRODE
L1 POSITIONER
POSITIONER

FIG.3

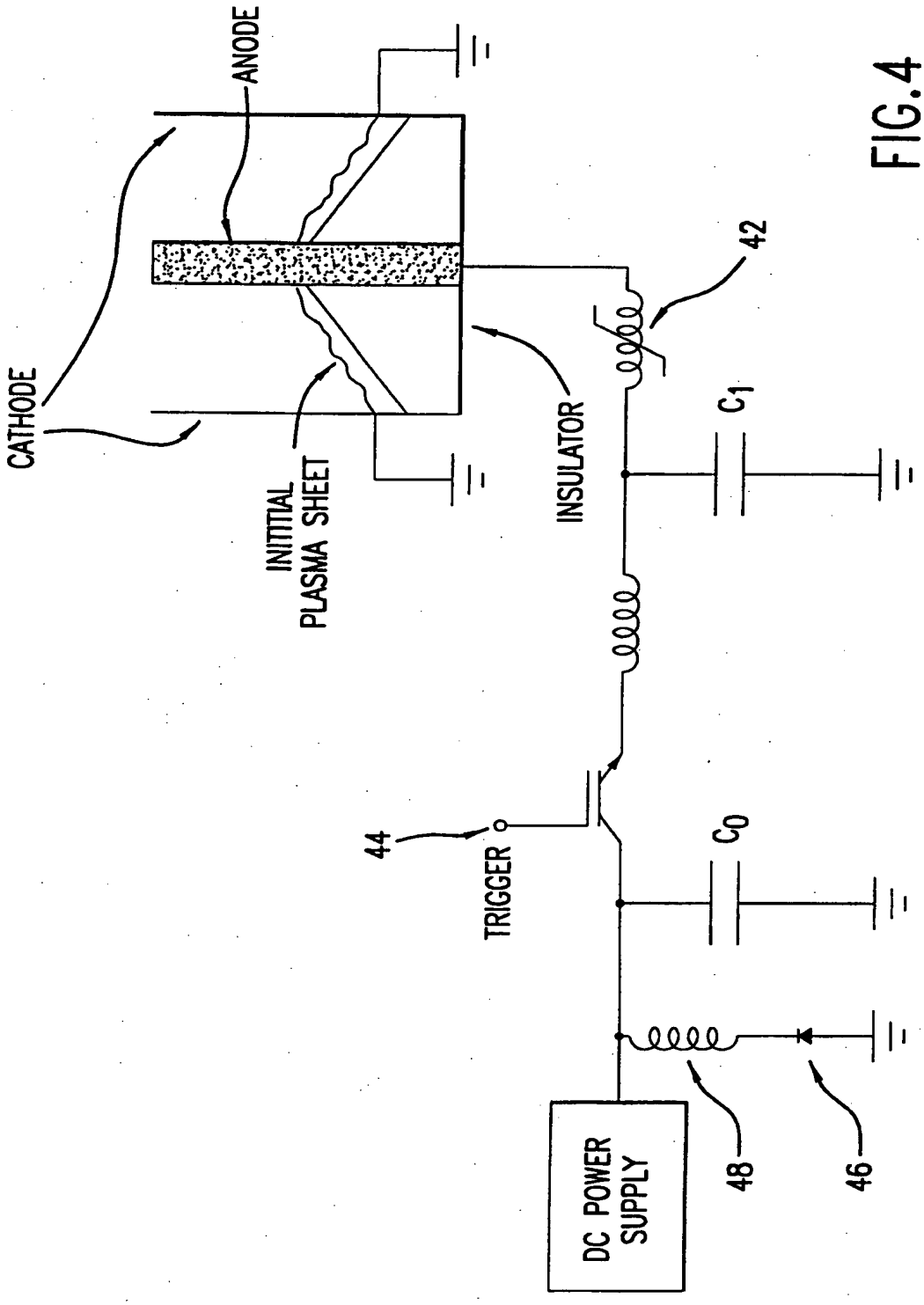
ANODE
CATHODE
INITITIAL PLASMA SHEET
INSULATOR
42
C_1
44
TRIGGER
C_0
DC POWER SUPPLY
48
46

FIG.4

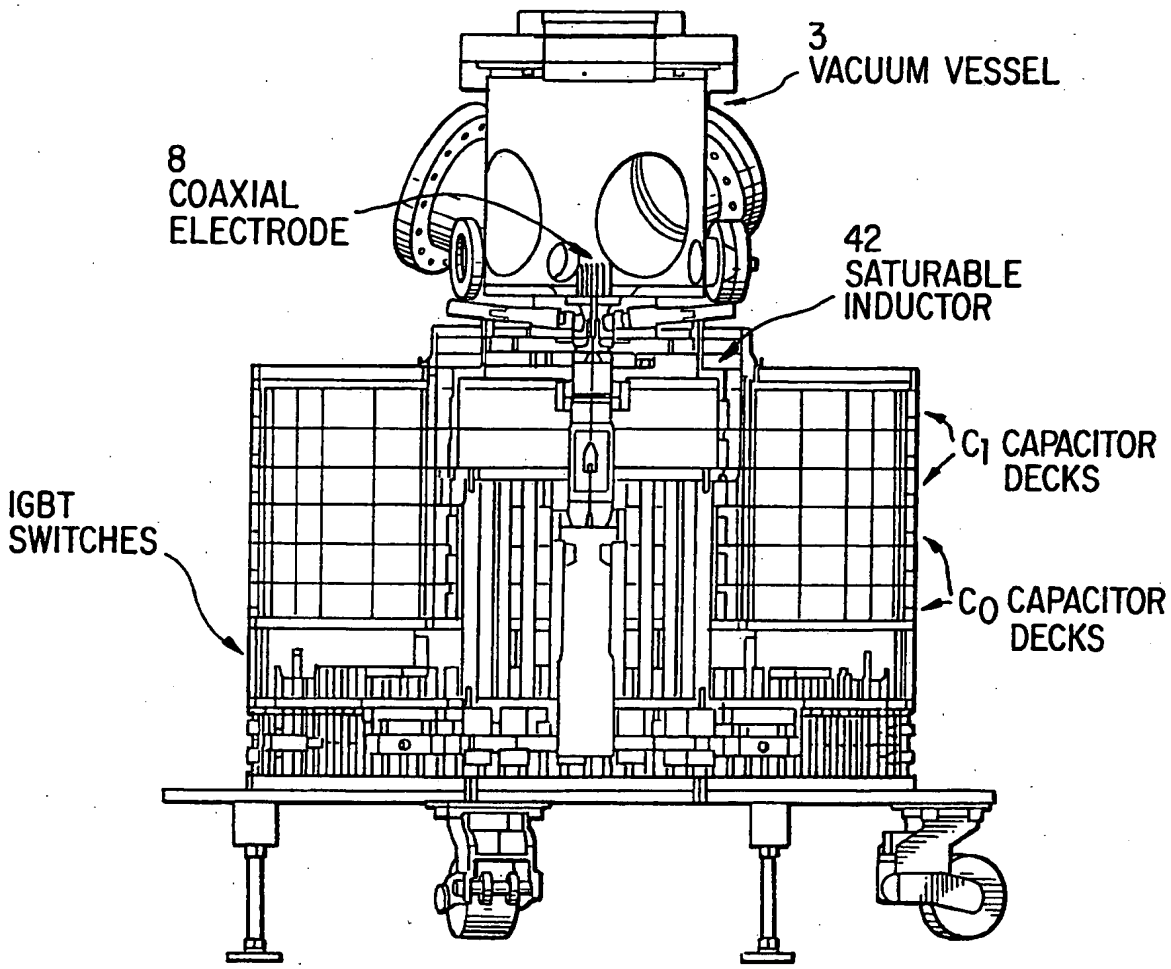
3
VACUUM VESSEL
8
COAXIAL
ELECTRODE
42
SATURABLE
INDUCTOR
C_1 CAPACITOR
DECKS
IGBT
SWITCHES
C_0 CAPACITOR
DECKS

FIG. 5A

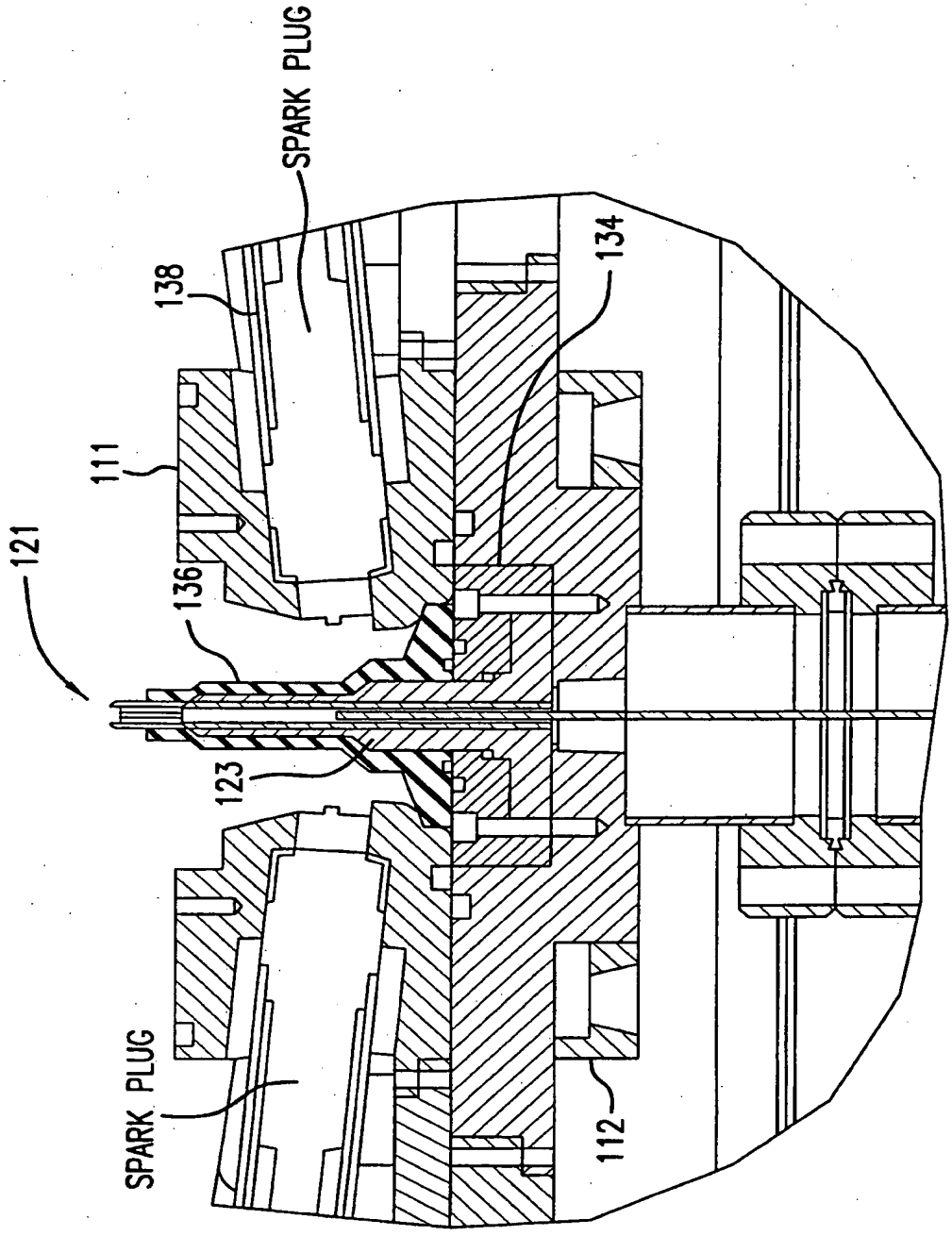

FIG. 5B

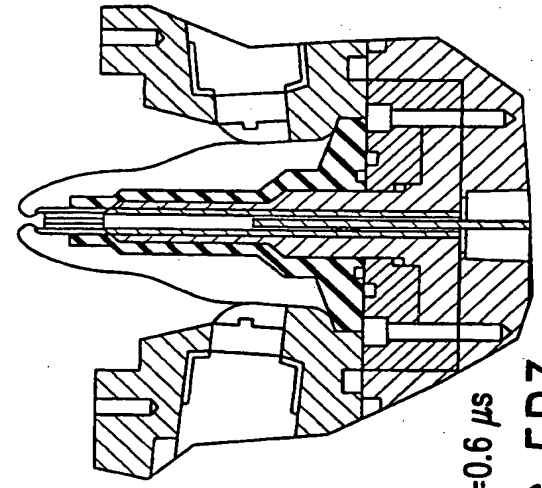

FIG. 5B1

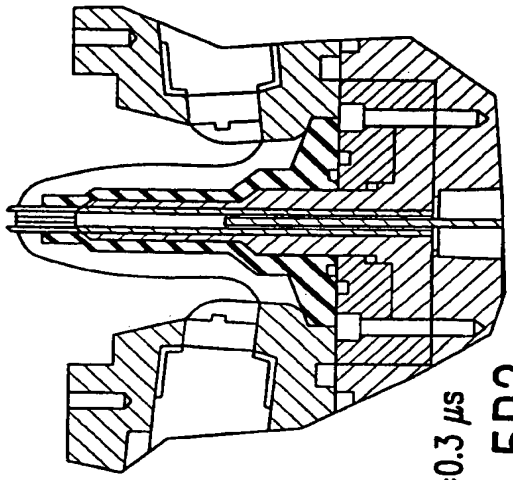

FIG. 5B2

FIG. 5B3

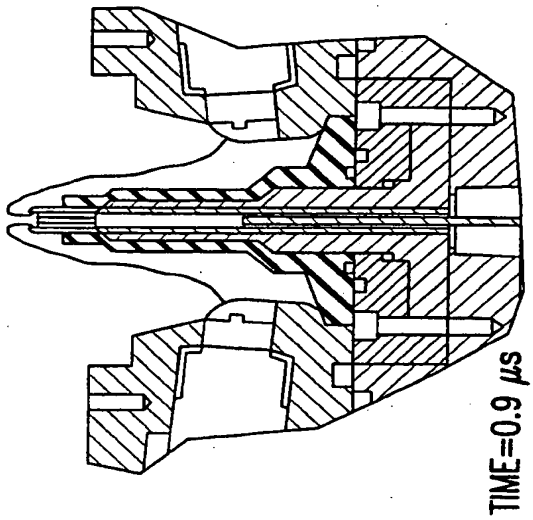

FIG. 5B4

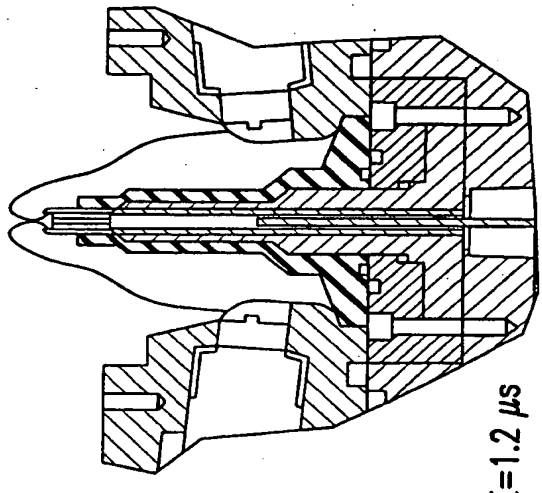

FIG. 5B5

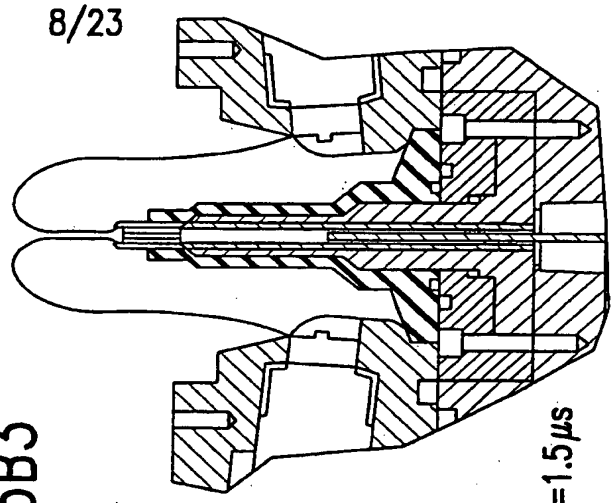

FIG. 5B6

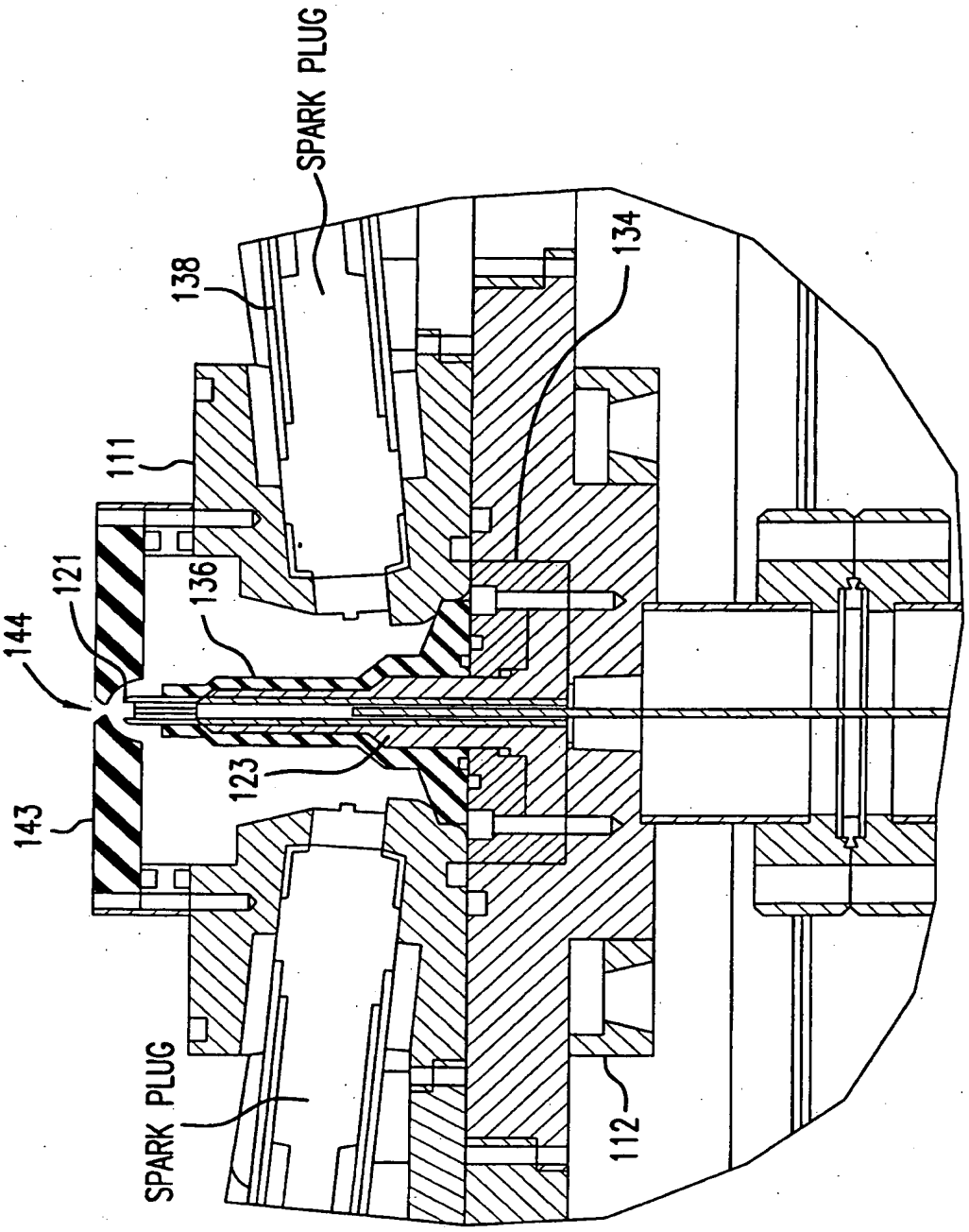

FIG. 5C

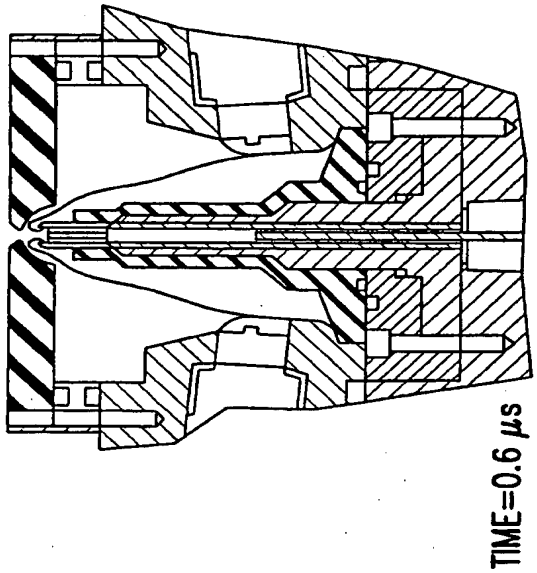

FIG. 5C3

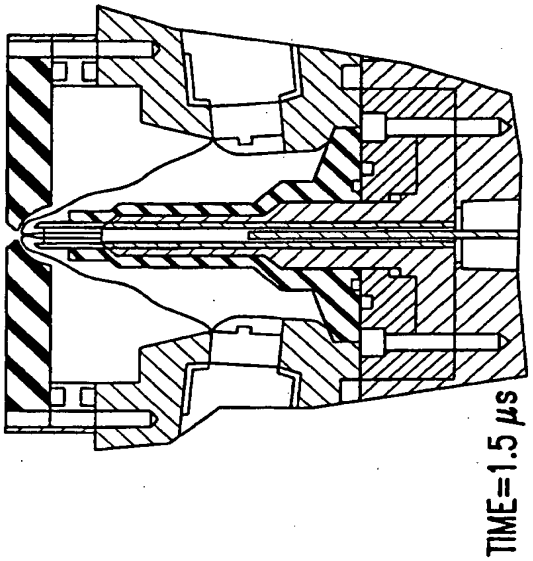

FIG. 5C6

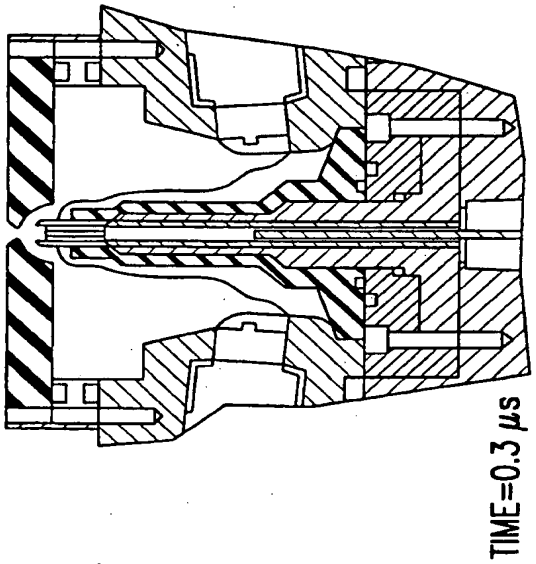

FIG. 5C2

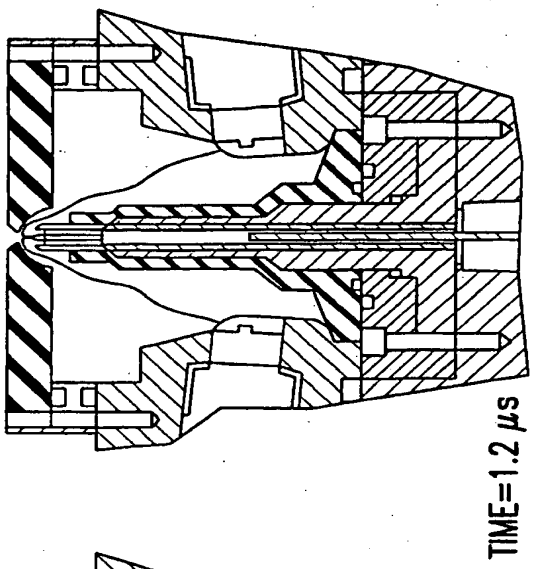

FIG. 5C5

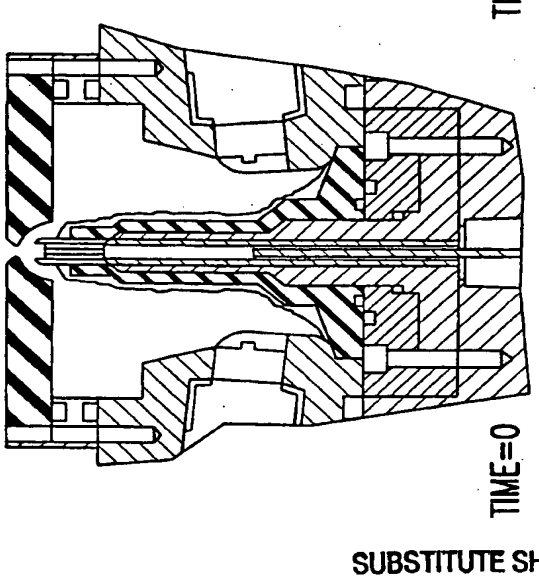

FIG. 5C1

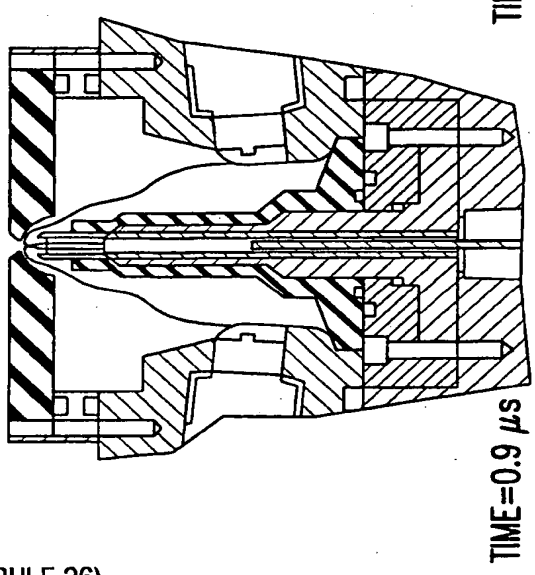

FIG. 5C4

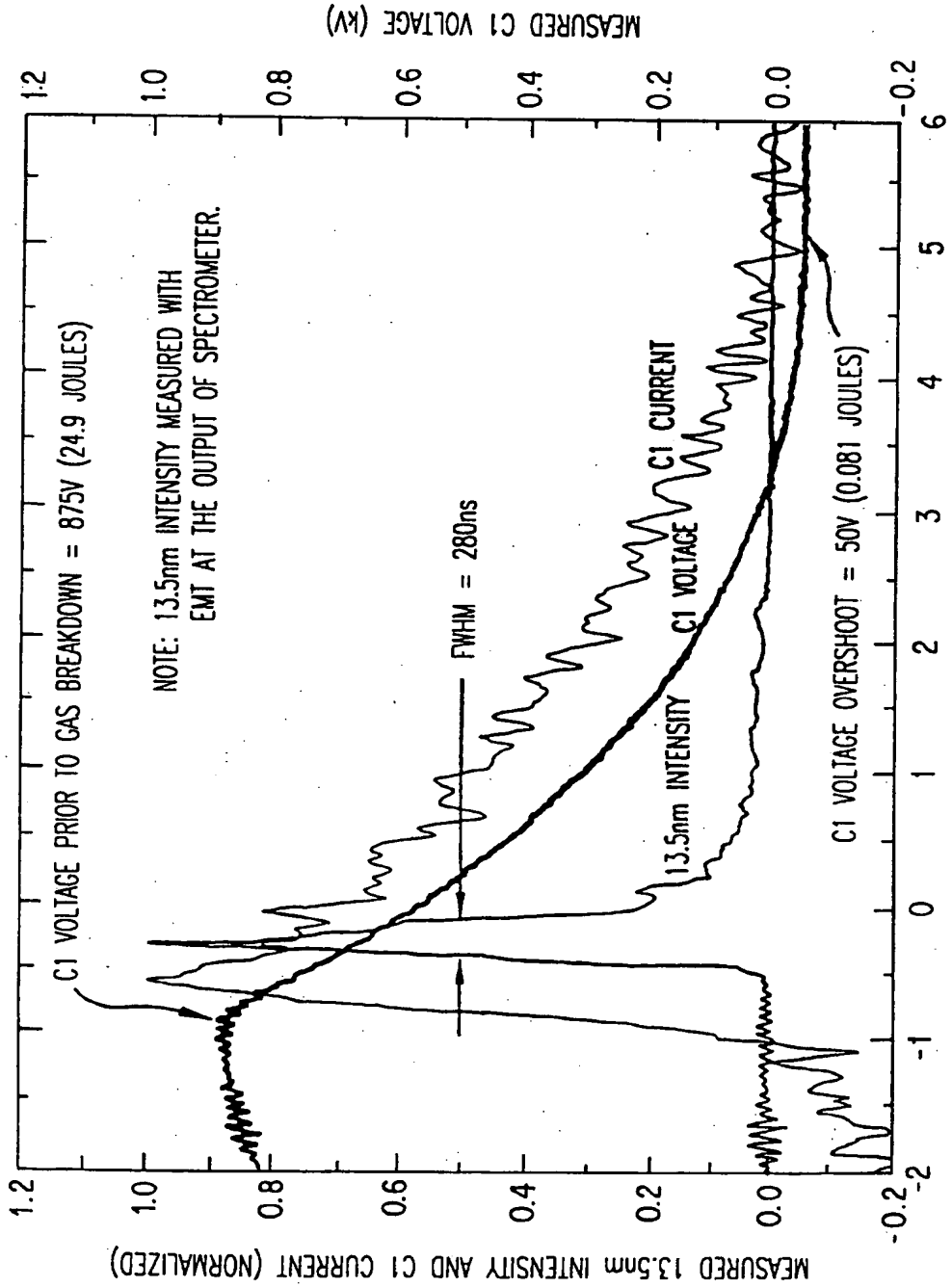
MEASURED C1 VOLTAGE (kV)
MEASURED 13.5nm INTENSITY AND C1 CURRENT (NORMALIZED)
TIME (μs)
C1 VOLTAGE PRIOR TO GAS BREAKDOWN = 875V (24.9 JOULES)
NOTE: 13.5nm INTENSITY MEASURED WITH EMT AT THE OUTPUT OF SPECTROMETER.
FWHM = 280ns
C1 CURRENT
C1 VOLTAGE
13.5nm INTENSITY
C1 VOLTAGE OVERSHOOT = 50V (0.081 JOULES)

FIG. 6

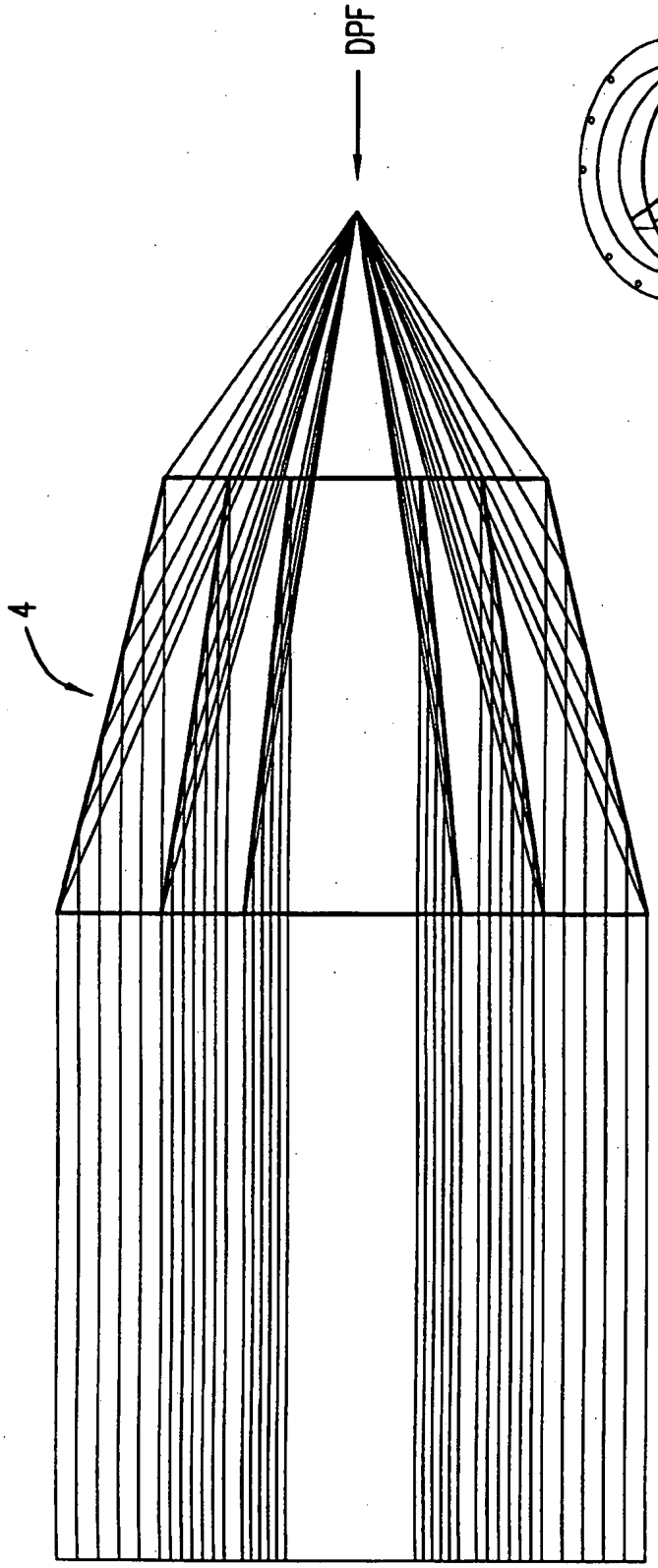

FIG. 7

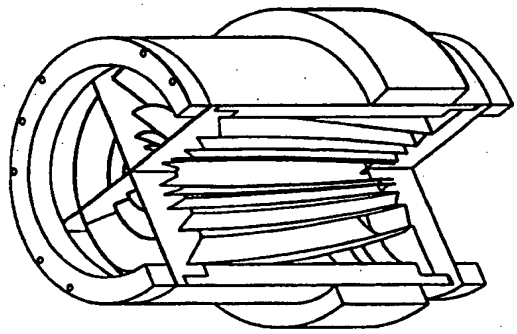

FIG. 7A

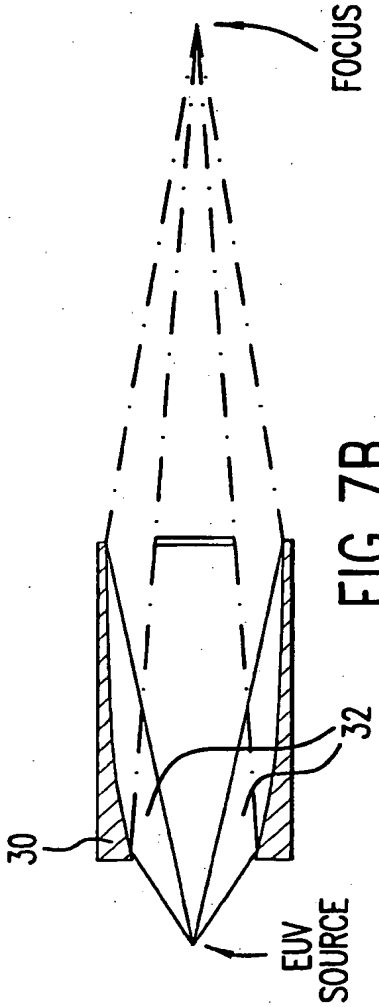

FIG. 7B

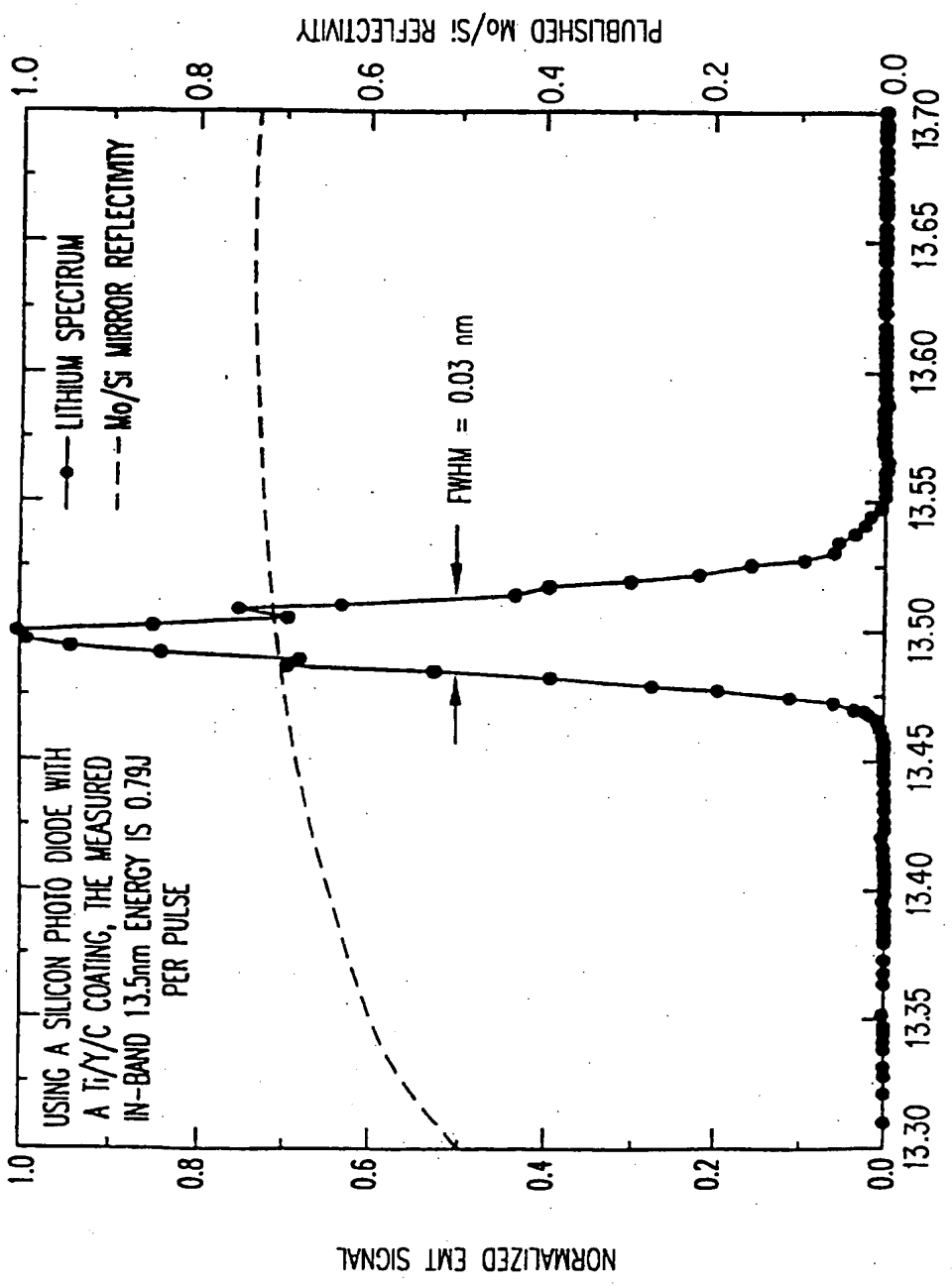
PLUBLISHED Mo/Si REFLECTIVITY
1.0
0.8
0.6
0.4
0.2
0.0
LITHIUM SPECTRUM
Mo/Si MIRROR REFLECTIVITY
FWHM = 0.03 nm
USING A SILICON PHOTO DIODE WITH
A Ti/Y/C COATING, THE MEASURED
IN-BAND 13.5nm ENERGY IS 0.79J
PER PULSE
NORMALIZED EMT SIGNAL
13.30
13.35
13.40
13.45
13.50
13.55
13.60
13.65
13.70
WAVELENGTH (nm)

FIG.8

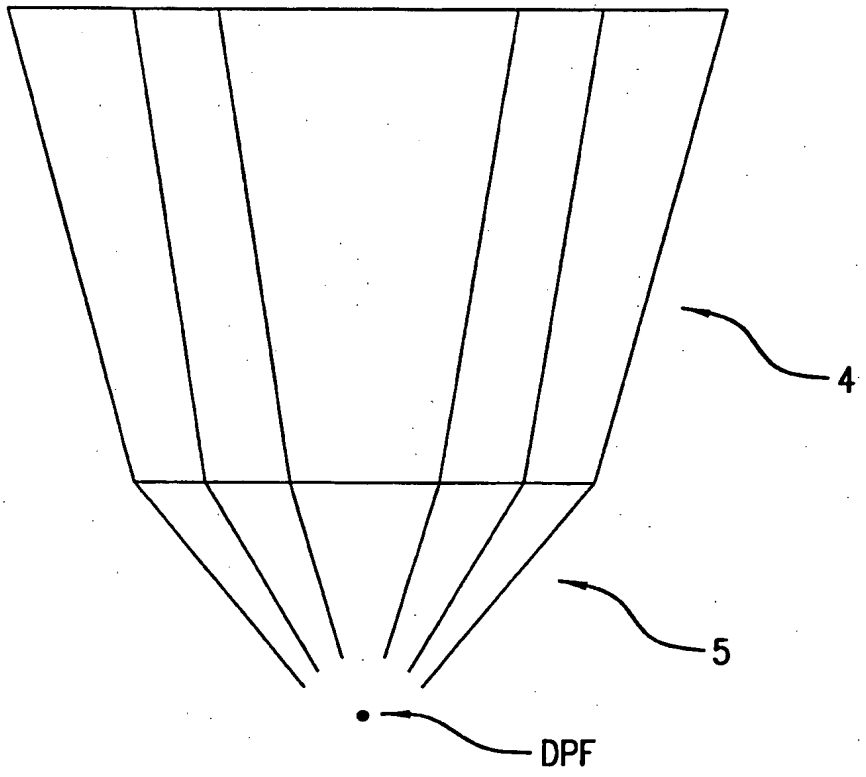

FIG.9

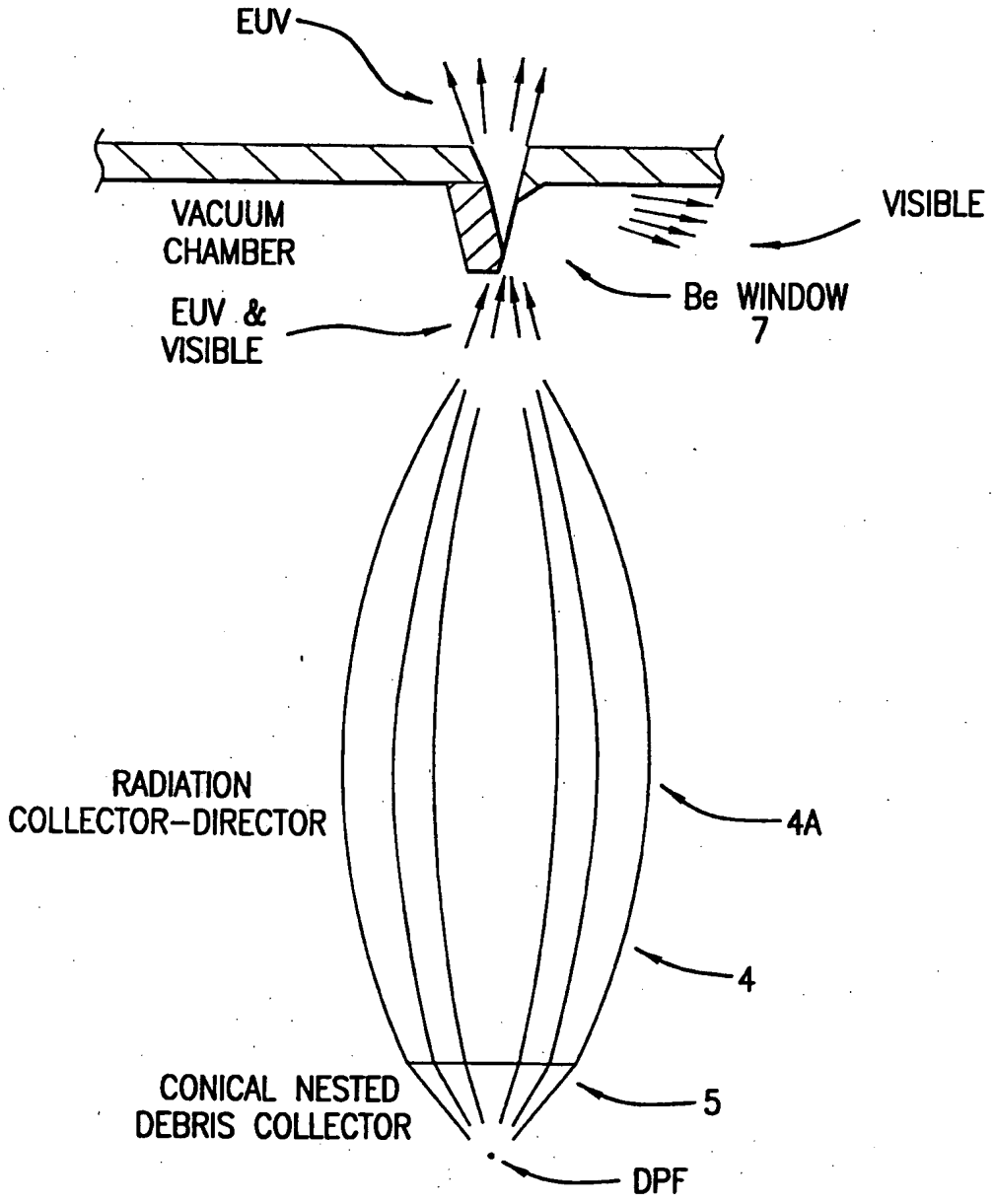
EUV
VACUUM CHAMBER
VISIBLE
Be WINDOW 7
EUV & VISIBLE
RADIATION COLLECTOR–DIRECTOR
4A
4
CONICAL NESTED DEBRIS COLLECTOR
5
DPF

FIG.10

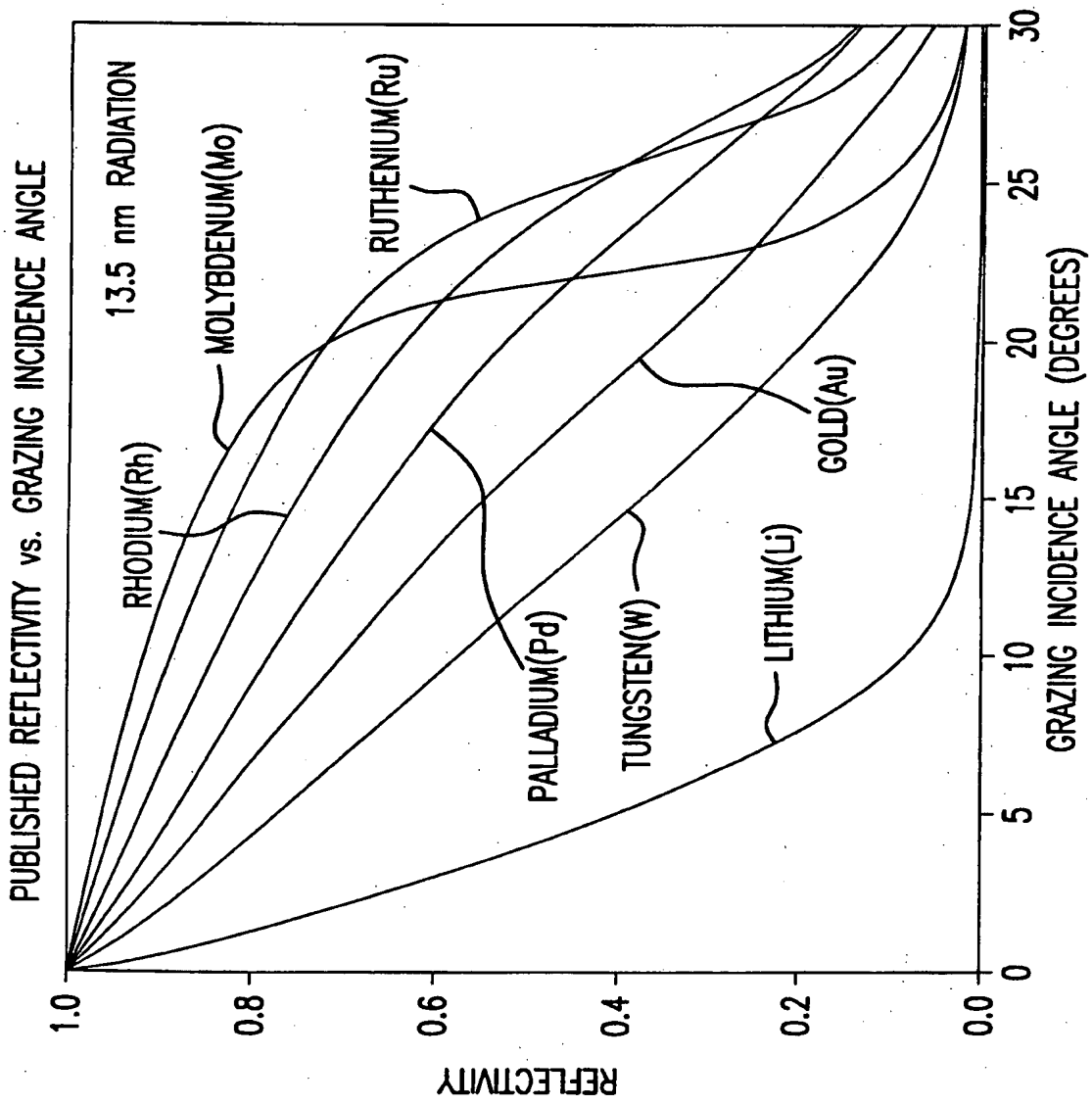
PUBLISHED REFLECTIVITY vs. GRAZING INCIDENCE ANGLE
13.5 nm RADIATION
RHODIUM(Rh)
MOLYBDENUM(Mo)
RUTHENIUM(Ru)
PALLADIUM(Pd)
TUNGSTEN(W)
LITHIUM(Li)
GOLD(Au)
REFLECTIVITY
1.0
0.8
0.6
0.4
0.2
0.0
0
5
10
15
20
25
30
GRAZING INCIDENCE ANGLE (DEGREES)

FIG. 11

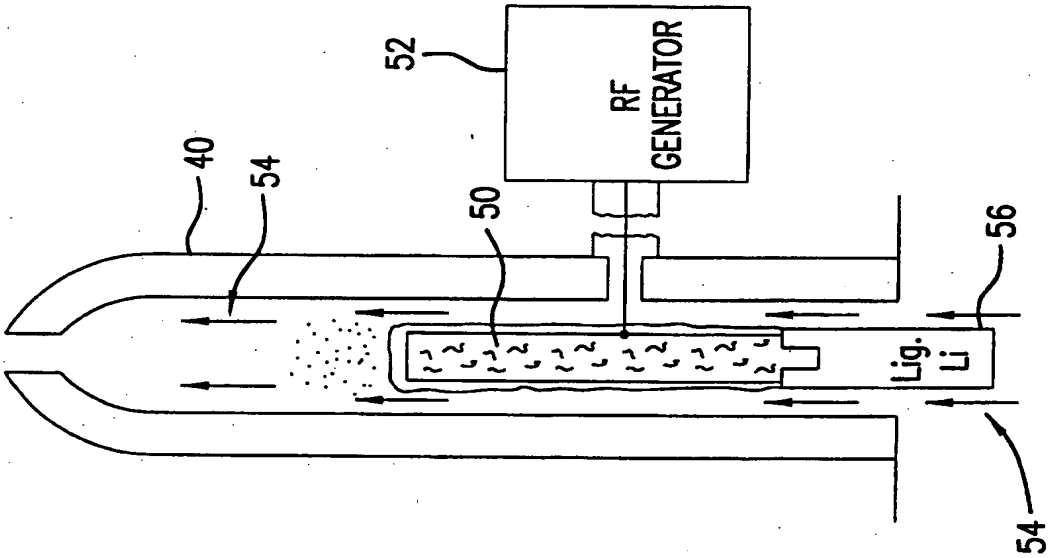

FIG. 15

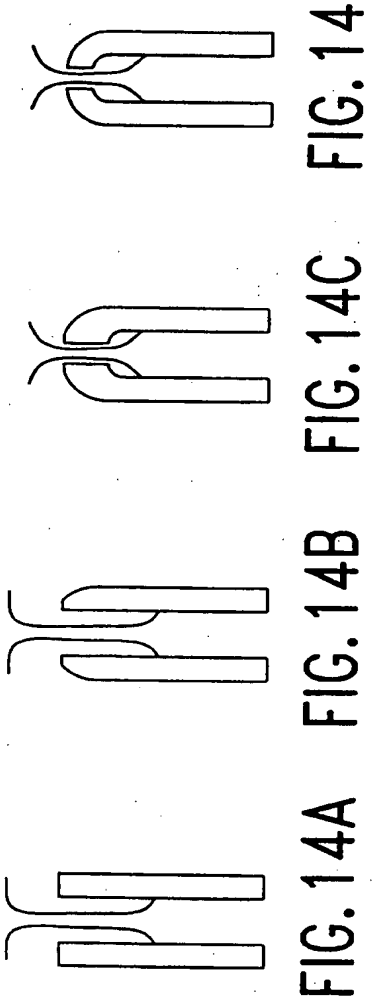

FIG. 14A FIG. 14B FIG. 14C FIG. 14D

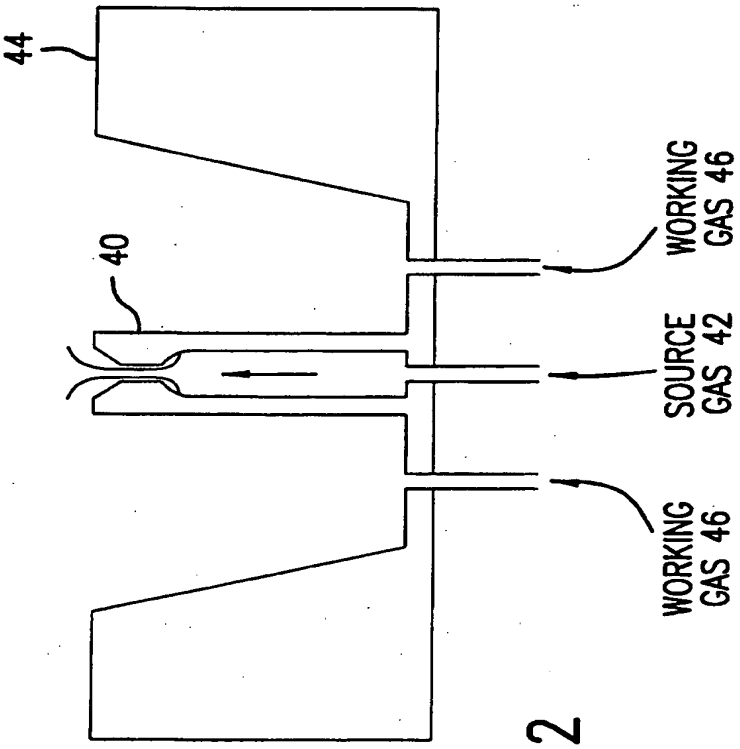

FIG. 12

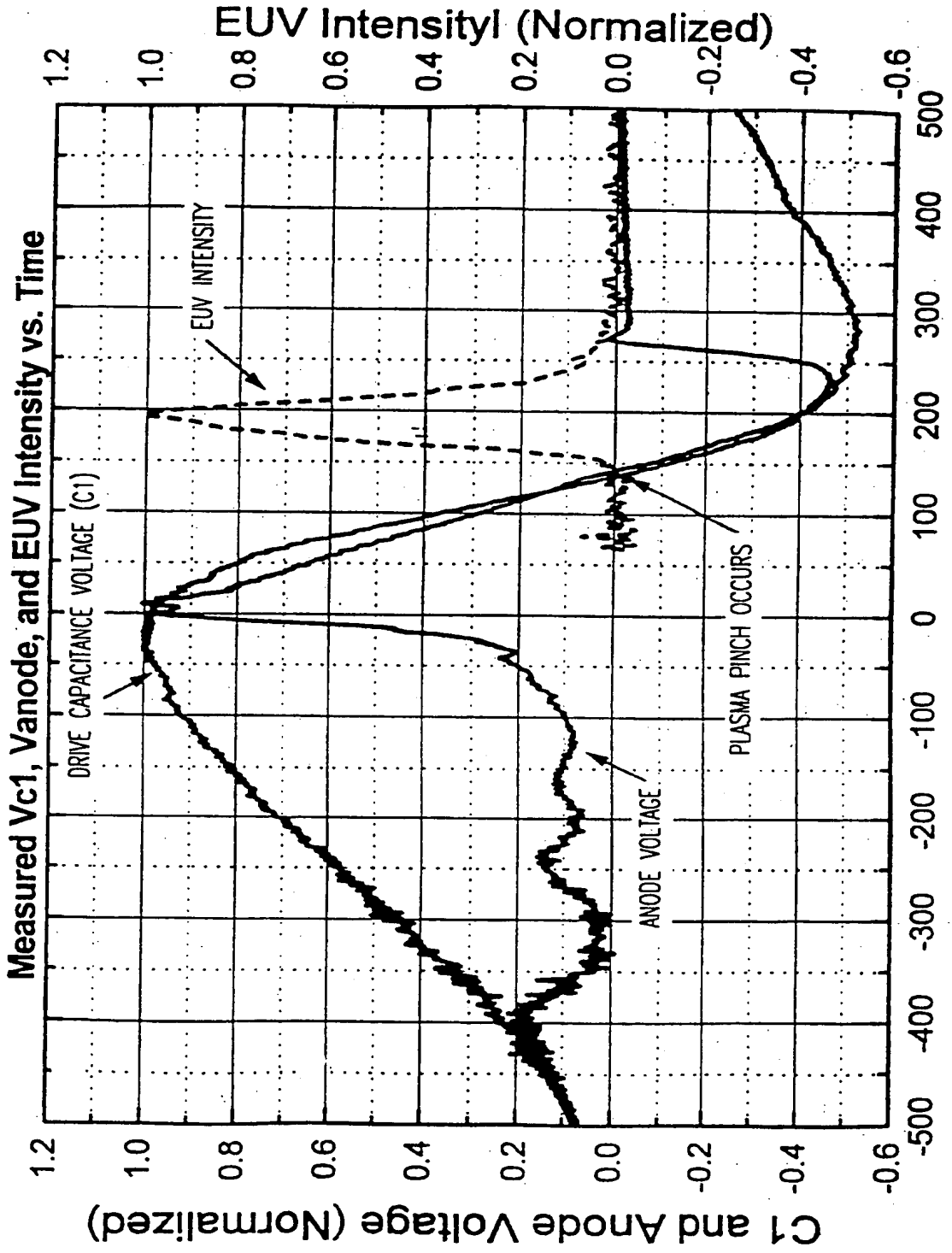
Measured Vc1, Vanode, and EUV Intensity vs. Time
EUV Intensityl (Normalized)
C1 and Anode Voltage (Normalized)
Time (ns)
EUV INTENSITY
DRIVE CAPACITANCE VOLTAGE (C1)
ANODE VOLTAGE
PLASMA PINCH OCCURS
1.2
1.0
0.8
0.6
0.4
0.2
0.0
-0.2
-0.4
-0.6
500
400
300
200
100
0
-100
-200
-300
-400
-500

FIG. 13

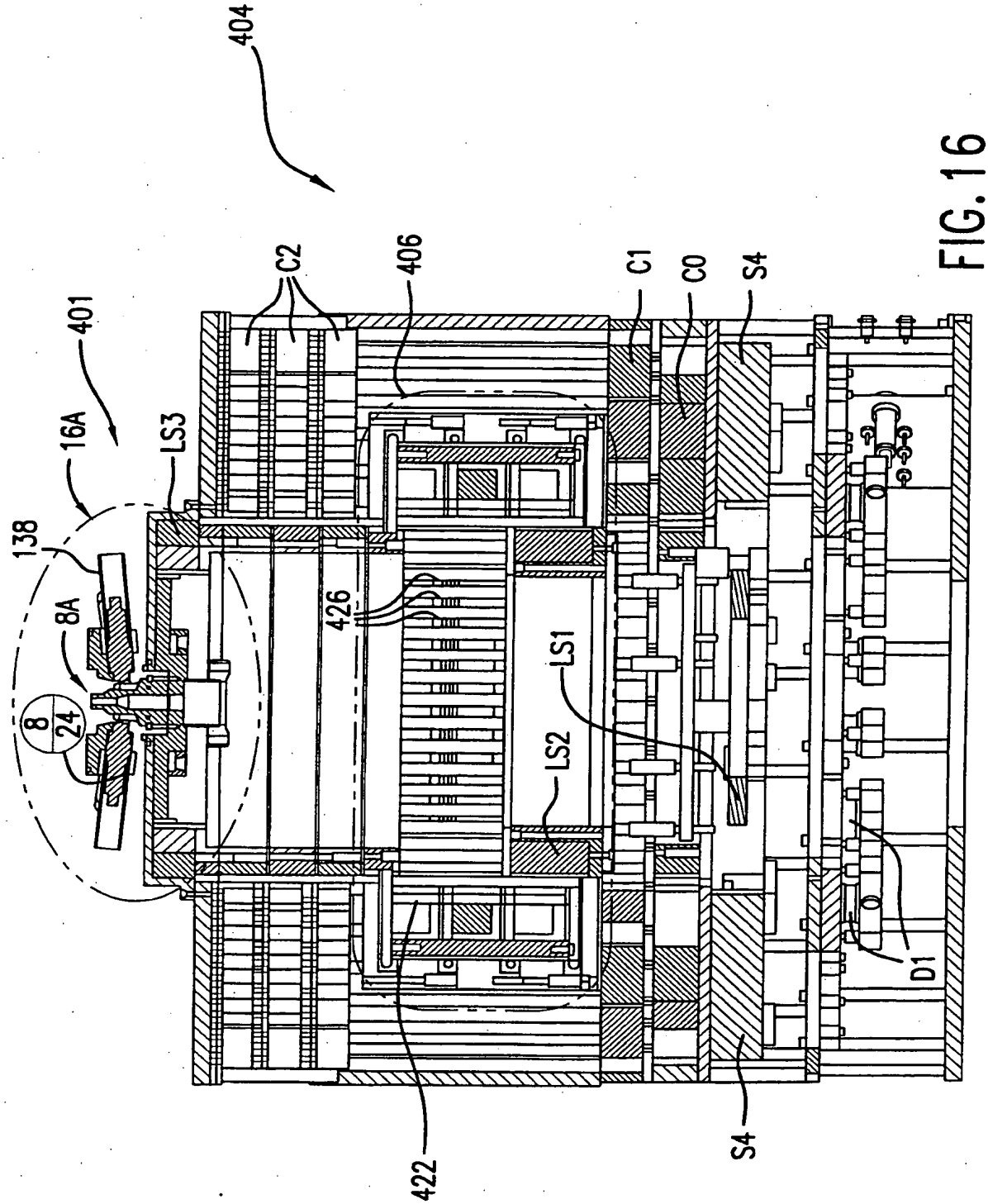

FIG. 16

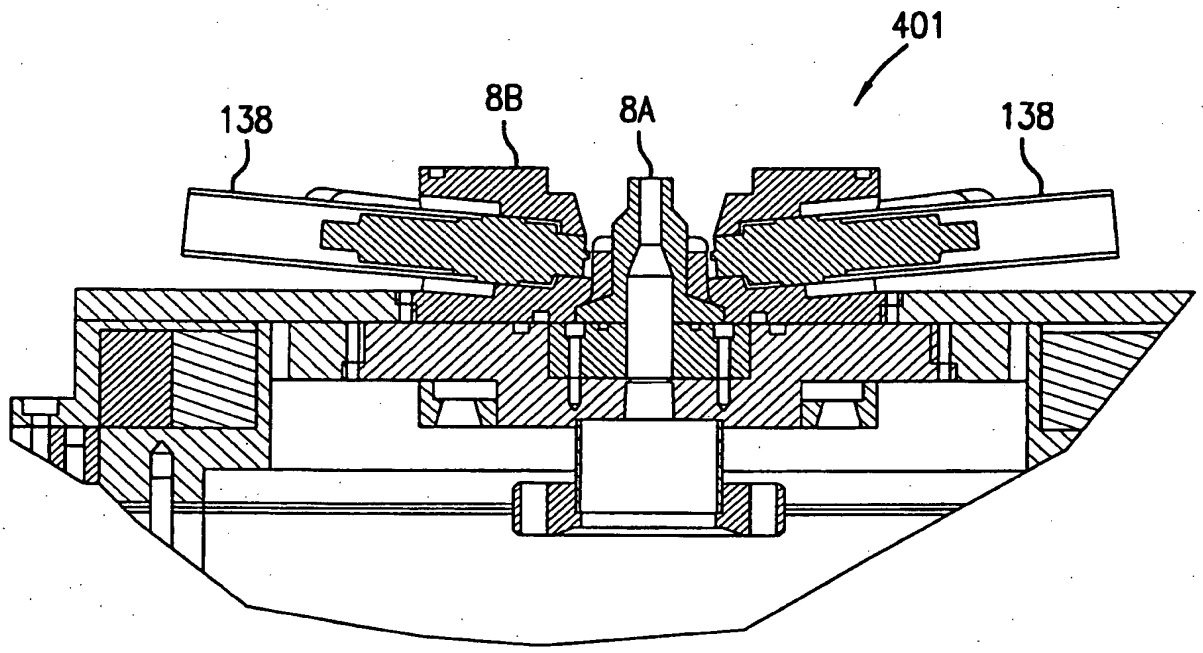

FIG. 16A

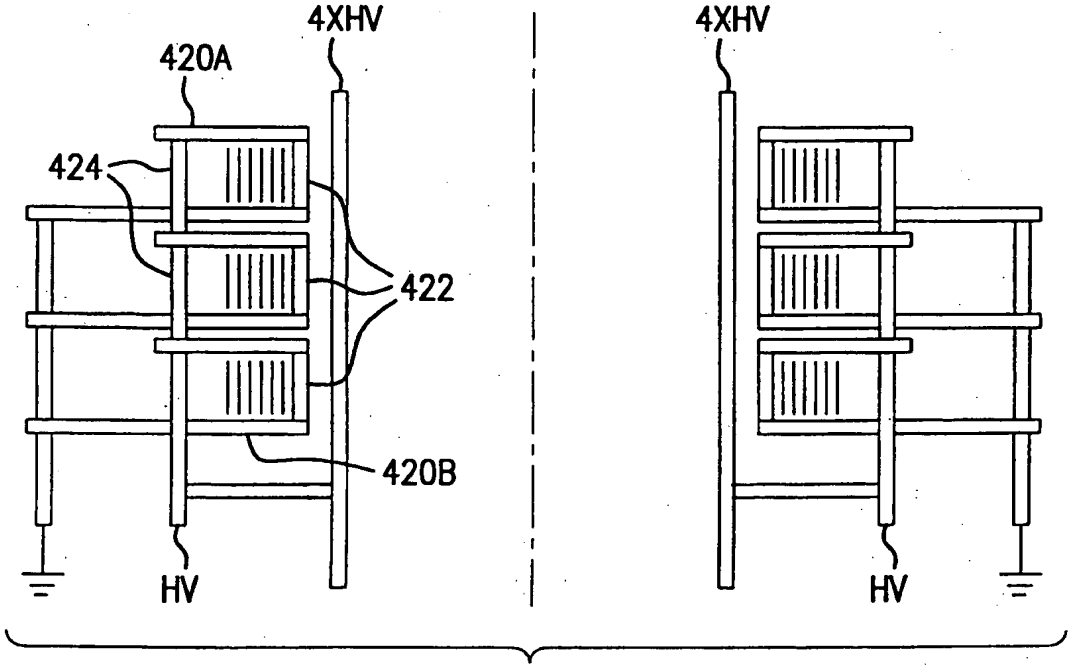

FIG. 16C

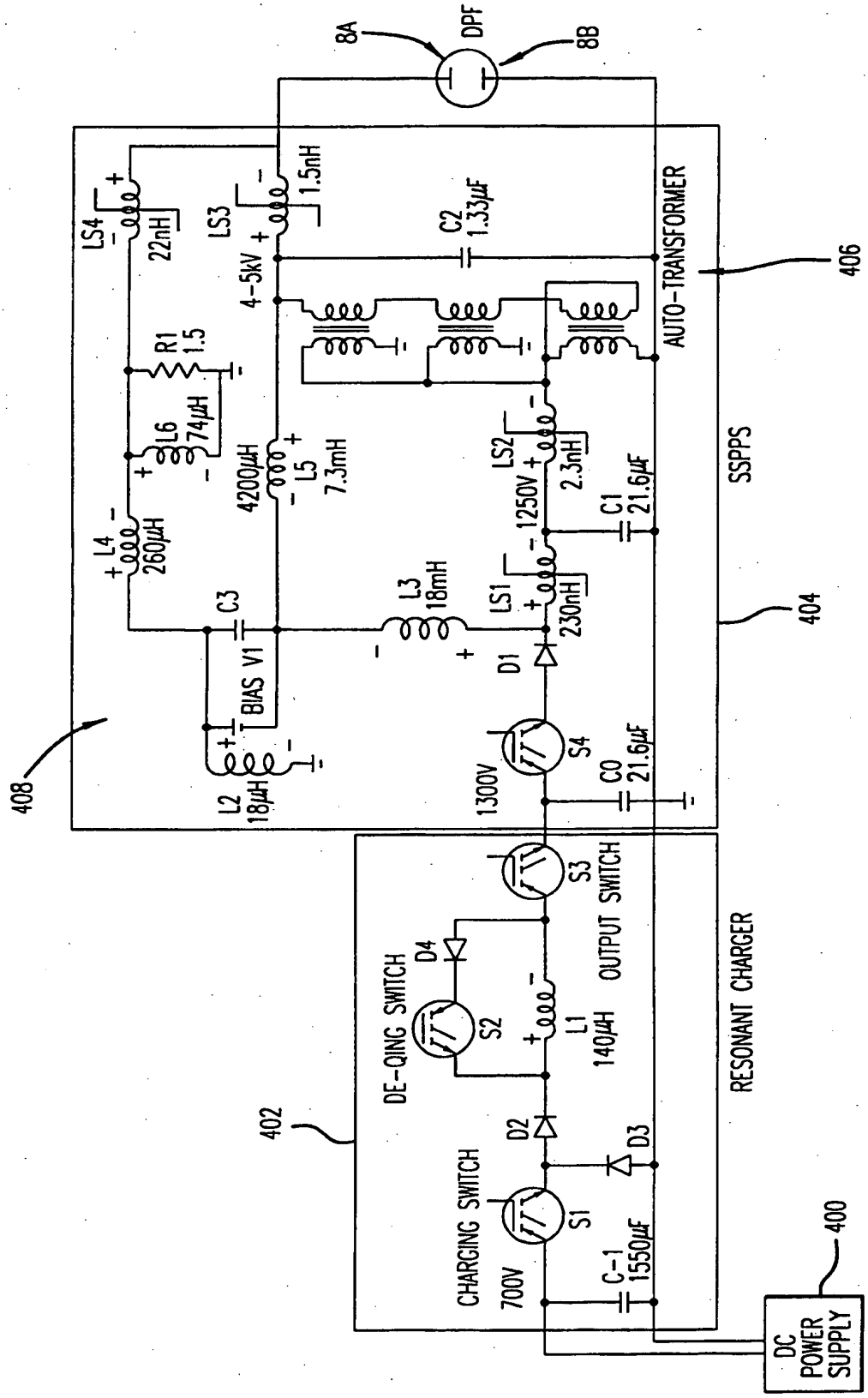
8A
DPF
8B
LS4
22nH
LS3
1.5nH
C2
1.33μF
4-5kV
AUTO-TRANSFORMER
406
R1
1.5
L6
74μH
420μH
L5
7.3mH
LS2
2.3nH
1250V
C1
21.6μF
SSPPS
L4
260μH
L3
18mH
LS1
230nH
C3
BIAS V1
D1
404
408
L2
18μH
1300V
S4
C0
21.6μF
S3
OUTPUT SWITCH
D4
DE-QING SWITCH
S2
L1
140μH
RESONANT CHARGER
402
D2
D3
CHARGING SWITCH
S1
700V
C-1
1550μF
400
DC
POWER
SUPPLY

FIG. 16B

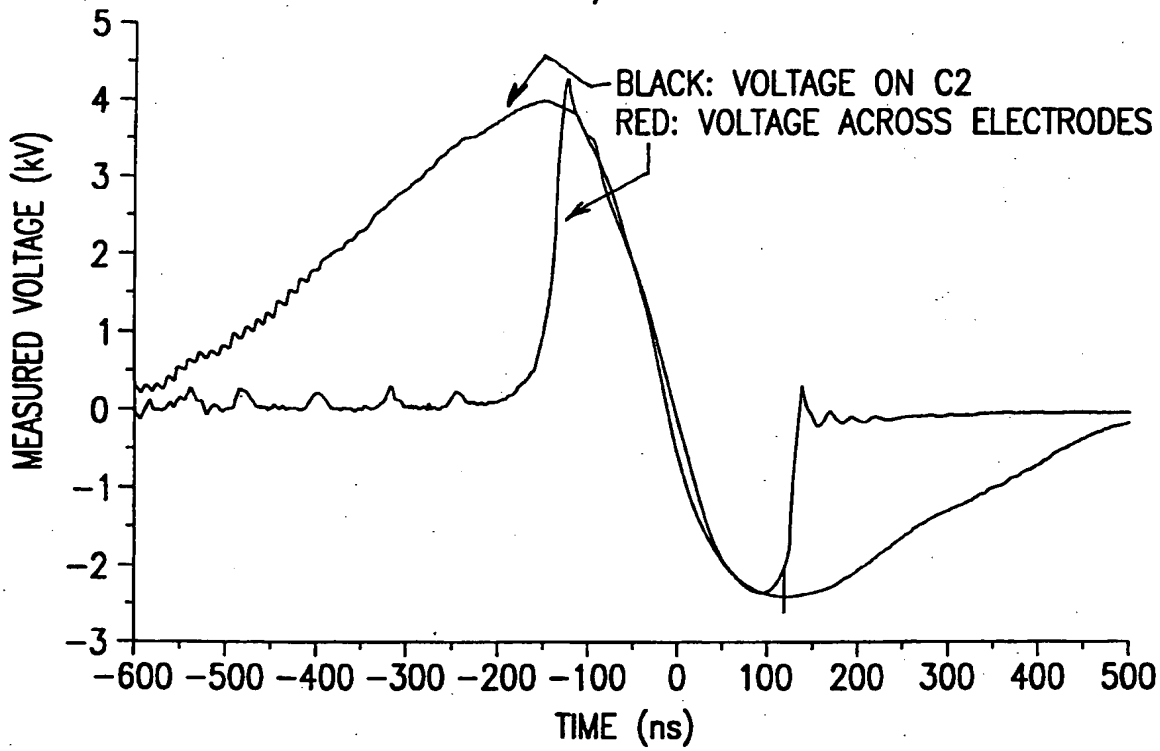

FIG. 16D

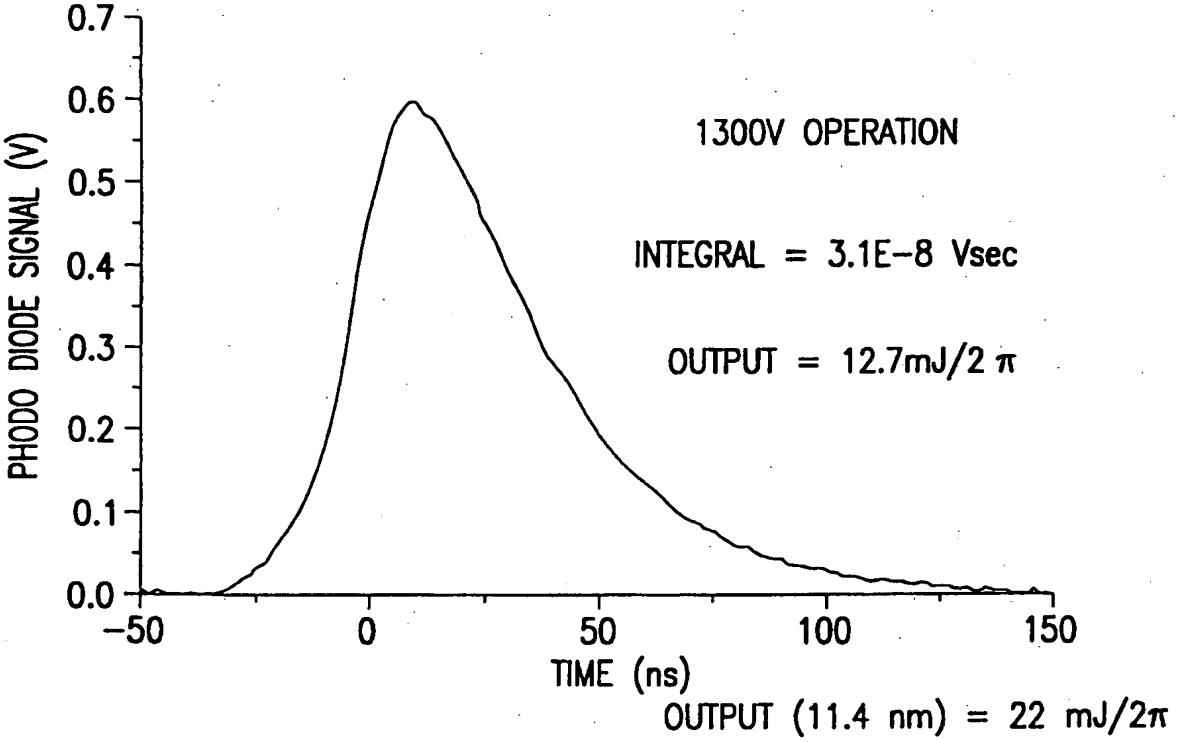

FIG. 16E

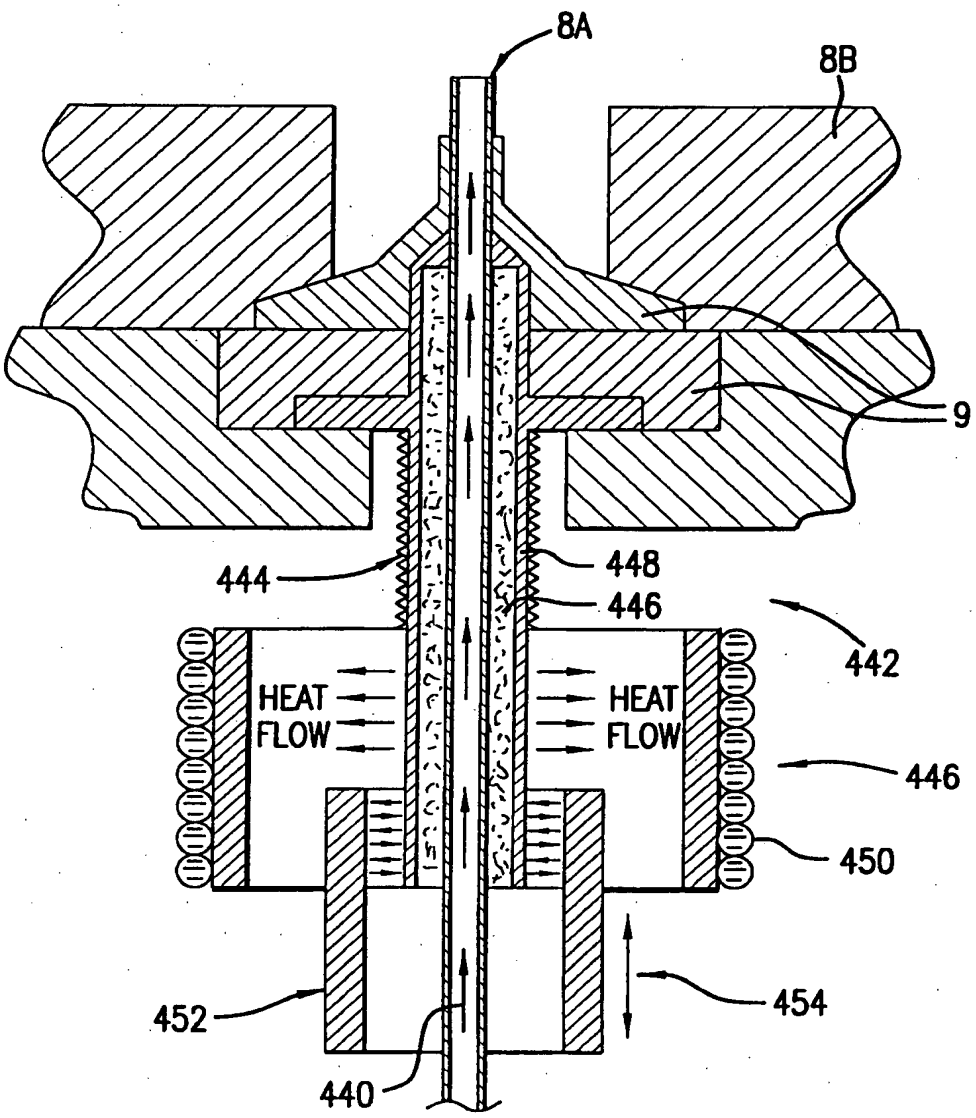

FIG. 17

INTERNATIONAL SEARCH REPORT

International application No.
PCT/US00/29750

A. CLASSIFICATION OF SUBJECT MATTER
IPC(7) :H01J 35/20; H01S 3/00, 3/22
US CL :250/504 R, 493.1; 372/28, 37, 38, 56, 81, 82
According to International Patent Classification (IPC) or to both national classification and IPC

B. FIELDS SEARCHED

Minimum documentation searched (classification system followed by classification symbols)
U.S. : 250/504 R, 493.1; 372/28, 37, 38, 56, 81, 82

Documentation searched other than minimum documentation to the extent that such documents are included in the fields searched
NONE

Electronic data base consulted during the international search (name of data base and, where practicable, search terms used)
EAST

C. DOCUMENTS CONSIDERED TO BE RELEVANT

Category*	Citation of document, with indication, where appropriate, of the relevant passages	Relevant to claim No.
X,P	US 6,064,072 A (PARTLO et al.) 16 May 2000 (16.05.2000), abstract and columns 3-10.	1-16
Y	US 5,313,481 A (COOK et al.) 17 May 1994 (17.05.1994), abstract and columns 8, 10.	17-23
Y	US 5,126,638 A (DETHLEFSEN) 30 June 1992 (30.06.1992), abstract and columns 5, 13-15.	17-19
Y	US 5,448,580 A (BIRX et al.) 05 September 1995 (05.09.1995), columns 3-5, 8, and 14.	20-23

☐ Further documents are listed in the continuation of Box C. ☐ See patent family annex.

* Special categories of cited documents:
"A" document defining the general state of the art which is not considered to be of particular relevance
"E" earlier document published on or after the international filing date
"L" document which may throw doubts on priority claim(s) or which is cited to establish the publication date of another citation or other special reason (as specified)
"O" document referring to an oral disclosure, use, exhibition or other means
"P" document published prior to the international filing date but later than the priority date claimed
"T" later document published after the international filing date or priority date and not in conflict with the application but cited to understand the principle or theory underlying the invention
"X" document of particular relevance; the claimed invention cannot be considered novel or cannot be considered to involve an inventive step when the document is taken alone
"Y" document of particular relevance; the claimed invention cannot be considered to involve an inventive step when the document is combined with one or more other such documents, such combination being obvious to a person skilled in the art
"&" document member of the same patent family

Date of the actual completion of the international search	Date of mailing of the international search report
14 DECEMBER 2000	16 JAN 2001
Name and mailing address of the ISA/US Commissioner of Patents and Trademarks Box PCT Washington, D.C. 20231 Facsimile No. (703) 305-3230	Authorized officer Sharon S. Hoppe ANTHONY G. QUASH Telephone No. (703) 308-0956

Form PCT/ISA/210 (second sheet) (July 1998) ★